Contents lists available at ScienceDirect

European Journal of Medicinal Chemistry

journal homepage: www.elsevier.com/locate/ejmech

Research paper

New aryl and acylsulfonamides as state-dependent inhibitors of Na$_v$1.3 voltage-gated sodium channel

Nace Zidar [a,*], Tihomir Tomašič [a], Danijel Kikelj [a], Martina Durcik [a], Jan Tytgat [b], Steve Peigneur [b], Marc Rogers [c], Alexander Haworth [c], Robert W. Kirby [c]

[a] University of Ljubljana, Faculty of Pharmacy, Aškerčeva cesta 7, 1000, Ljubljana, Slovenia
[b] University of Leuven (KU Leuven), Toxicology & Pharmacology, O&N2, PO Box 922, Herestraat 49, 3000, Leuven, Belgium
[c] Metrion Biosciences Limited, Building 2, Granta Centre, Granta Park, Great Abington, Cambridge, CB21 6AL, UK

ARTICLE INFO

ABSTRACT

Voltage-gated sodium channels (Na$_v$s) play an essential role in neurotransmission, and their dysfunction is often a cause of various neurological disorders. The Na$_v$1.3 isoform is found in the CNS and upregulated after injury in the periphery, but its role in human physiology has not yet been fully elucidated. Reports suggest that selective Na$_v$1.3 inhibitors could be used as novel therapeutics to treat pain or neurodevelopmental disorders. Few selective inhibitors of this channel are known in the literature. In this work, we report the discovery of a new series of aryl and acylsulfonamides as state-dependent inhibitors of Na$_v$1.3 channels. Using a ligand-based 3D similarity search and subsequent hit optimization, we identified and prepared a series of 47 novel compounds and tested them on Na$_v$1.3, Na$_v$1.5, and a selected subset also on Na$_v$1.7 channels in a QPatch patch-clamp electrophysiology assay. Eight compounds had an IC$_{50}$ value of less than 1 μM against the Na$_v$1.3 channel inactivated state, with one compound displaying an IC$_{50}$ value of 20 nM, whereas activity against the inactivated state of the Na$_v$1.5 channel and Na$_v$1.7 channel was approximately 20-fold weaker. None of the compounds showed use-dependent inhibition of the cardiac isoform Na$_v$1.5 at a concentration of 30 μM. Further selectivity testing of the most promising hits was measured using the two-electrode voltage-clamp method against the closed state of the Na$_v$1.1-Na$_v$1.8 channels, and compound **15b** displayed small, yet selective, effects against the Na$_v$1.3 channel, with no activity against the other isoforms. Additional selectivity testing of promising hits against the inactivated state of the Na$_v$1.3, Na$_v$1.7, and Na$_v$1.8 channels revealed several compounds with robust and selective activity against the inactivated state of the Na$_v$1.3 channel among the three isoforms tested. Moreover, the compounds were not cytotoxic at a concentration of 50 μM, as demonstrated by the assay in human HepG2 cells (hepatocellular carcinoma cells). The novel state-dependent inhibitors of Na$_v$1.3 discovered in this work provide a valuable tool to better evaluate this channel as a potential drug target.

1. Introduction

Voltage-gated sodium channels (Na$_v$s) are transmembrane proteins that open and close in response to membrane potential, controlling the flux of sodium ions from the extracellular to the intracellular side [1–3]. They are expressed in various electrically excitable cells where they are responsible for electrical signalling. The main part of the channels consists of a large α-subunit with four homologous domains, DI-DIV, arranged to form a central pore. Each of the domains contains a voltage-sensor domain (VSD) consisting of four transmembrane helices, S1–S4, which responds to changes in membrane potential and affects the

functional state of the channel [4]. Although the α-subunit alone is sufficient for ion conduction, it is usually associated with one or more β-subunits that regulate the kinetics of channel gating, cell surface expression or act as adhesion molecules [5]. There are nine known members of the Na$_v$1 channel family, Na$_v$1.1–Na$_v$1.9, with different functional properties and expression patterns in cells, such as peripheral and central neurons (Na$_v$1.1–1.3 and 1.6–1.9), skeletal muscles (Na$_v$1.4), and cardiac muscle (Na$_v$1.5) [2].

Na$_v$ channels exist in three main functional states: closed (resting), open, and inactivated [1]. The affinities of Na$_v$ channel inhibitors for each of these states are often different. Many known inhibitors block

---

* Corresponding author.
   E-mail address: nace.zidar@ffa.uni-lj.si (N. Zidar).

preferentially the open or inactivated state, which is referred to as a state-dependent action. Additionally, many compounds bind with higher affinity to channels in cells with higher firing frequencies, known as use dependence. State and use dependence are preferred properties of Na_v channel inhibitors, as this enhances their binding to damaged nerves with pathological firing patterns [3]. The abnormal activities of Na_v isoforms have been associated with various diseases, such as epilepsy (Na_v1.1, 1.2, 1.3, 1.6), periodic paralysis (Na_v1.4), cardiac arrhythmias (Na_v1.5), CNS tremor, ataxia and dystonia (Na_v1.6), and hyper- or hyposensitivity to pain (Na_v1.3, 1.7, 1.8, 1.9).

Early Na_v channel modulators, such as local anaesthetics (lidocaine, bupivacaine), anticonvulsants (carbamazepine), antiepileptics (phenytoin) and antiarrhythmics (mexiletine) were largely subtype nonselective. To avoid possible CNS (dizziness, sedation, convulsions) or cardiovascular (arrhythmias, cardiotoxicity) side effects, subtype-selective inhibitors are being investigated. However, due to the high degree of sequence similarity between Na_v subtypes, it is difficult to achieve subtype selectivity [3,4]. In recent years, the discovery of Na_v channel inhibitors has been facilitated by an advanced understanding of the biology and genetics of Na_v channels [6,7], new automated screening technologies [8], new heterologous ion channel expression systems [9], structural data of bacterial [10–14] and eukaryotic [5,15, 16] Na_v channels in various functional states, and co-crystal structures of Na_v channels with small molecules [17].

Na_v1.7, Na_v1.8, and Na_v1.9 channels have been identified as the major contributors to nociceptive signalling [4]. Of these channels, Na_v1.7 is the best studied and is considered a key player in pain reception. The role of Na_v1.3 is less well understood, but some studies suggest that it is also involved in pain pathways [18–21]. Na_v1.3 channels are mainly expressed in the CNS of the embryonic brain and their expression decreases significantly after birth [22]. However, it has been shown that nerve injury can lead to upregulation of Na_v1.3, resulting in neuronal hyperexcitability and pain [20,23]. In addition, Na_v1.3 is expressed in neutrophils and its inhibition may have anti-inflammatory effects [24]. Mutations in the *SCN3A* gene, which encodes the α-subunit of Na_v1.3, have been associated with neuro-developmental disorders, such as epilepsy and brain malformations [25–28].

One of the most important binding sites for the development of subtype-selective small molecule Na_v channel inhibitors that has emerged in recent years is located on the extracellular side of the fourth VSD [17,29,30]. The binding site lies between helices S2, S3, and S4 and is partially immersed in the membrane bilayer, as shown by mutational studies [30] and the crystal structure of a small molecule inhibitor bound to this site [17]. Inhibitors targeting this site belong to the structural class of aryl- and acylsulfonamides. The anionic arylsulfona-mide warhead of the inhibitors makes contacts with the fourth arginine of the S4 helix, while contacts with residues of the S2 and S3 helix are important to achieve isoform selectivity. Aryl- and acylsulfonamides bind to the inactivated state of the channel, stabilizing the voltage sensor in the activated (or "up") conformation and thus trapping the channel in the nonconducting inactivated state. They exhibit state- and use-dependent blockade.

Most aryl- and acylsulfonamides have been investigated as Na_v1.7 channel blockers for the treatment of pain and many of them show very good selectivity profiles over Na_v1.5 and other isoforms [31–36]. Several Na_v1.7 inhibitors have advanced through various stages of preclinical and clinical development [2,29,37]. However, despite their very high potency and selectivity, it has proven difficult to translate these compounds into successful therapeutics [38,39]. Many of the known inhibitors have poor drug metabolism and pharmacokinetic (DMPK) properties, poor blood–brain barrier permeability, and high plasma protein binding, so it remains difficult to achieve potent anal-gesic effects *in vivo* [32]. In addition to Na_v1.7, arylsulfonamides have also been investigated as Na_v1.3 inhibitors, and some of the reported compounds achieved good potency and isoform selectivity [16,30,40].

Given the recent discoveries demonstrating the important role of Na_v1.3 in human physiology, new potent and selective Na_v1.3 inhibitors are needed to better evaluate this channel as a potential drug target.

2. Results and discussion

Design. The design of the present series of compounds was based on the arylsulfonamide class of Na_v inhibitors that bind to the extracellular small molecule binding site on VSD4. Compounds **I** and **II** (Fig. 1) with IC_{50} values for human Na_v1.3 in the low nanomolar range served as starting points [41]. The extracellular VSD4 binding site has greater sequence diversity among different Na_v subtypes than the central pore region, making this site attractive for the development of subtype-selective Na_v inhibitors. The general design protocol is shown in Fig. 1. First, a computational approach was used with a ligand-based 3D similarity search. Compound **II** was used as a query, and the similarity search was performed on a drug-like subset of the ZINC library of compounds using a combination of ROCS and EON from OpenEye Sci-entific Software, Inc [42,43]. The obtained results were evaluated, and sixteen compounds (Table 3) were selected based on their calculated ET_Combo similarities (Supplementary information, Table 1S) and structural diversity, and purchased. In addition, new potential Na_v1.3 modulators were designed by systematic structural modifications of inhibitors **I** and **II** (type I compounds, Fig. 2). Moreover, an Icagen compound **III** [44] (Fig. 3), recently used by our research group to characterize endogenous sodium channels in the ND7-23 cell line [45], was used as a starting compound for the preparation of new analogues due to its high state-dependent activity against human Na_v1.3 (IC_{50} of 56 nM for the inactivated state and 18 µM for the resting state), and no effects on Na_v1.4, Na_v1.5, Na_v1.6, and Na_v1.7 [45]. The design strategy for new Na_v1.3 inhibitors based on the compound **III** is shown in Fig. 3 (type II compounds).

To facilitate the design of new compounds, inhibitors **I-III** were visually divided into three structural parts: (*i*) the substituted pyrazol-5-amine (**I** and **II**) or 2-phenylcyclopropane-1-carboxamide (**III**) on the left hand side (LHS, coloured red), (*ii*) the central benzene ring (coloured black), and (*iii*) the *N*-(thiazol-2-yl)sulfonamide moiety on the right hand side (RHS, coloured blue) (Fig. 2).

Subtype selectivity of inhibitors can be achieved primarily by vary-ing the LHS, which usually contains hydrophobic substituents. In the first series of analogues, the substituted pyrazol-5-amine moiety on the LHS was replaced by various substituted pyrrole-2-carboxamide moi-eties (types Ia-b, Fig. 2). Phenyl, benzyl, or substituted benzyl groups were attached to the pyrrole nitrogen to mimic the structure of the substituents of compounds **I** and **II**. In some analogues, positions 4 and 5 of the pyrrole ring were substituted by bromine atoms (types Ia-b, Fig. 2). The substitution pattern on the disubstituted central benzene ring was either 1,4 or 1,3 (type Ia, Fig. 2). The charged warhead at the RHS is critical for establishing interactions with the gating arginine at the VSD. Therefore, we retained the *N*-(thiazol-2-yl)sulfonamide moiety at this position for most analogues. In some compounds, an acetate group was introduced on the sulfonamide nitrogen in place of the thiazole group to determine whether the thiazole ring was essential for high binding affinity (type Ia, Fig. 2). In addition to the arylsulfonamides (types Ia and IIa, Figs. 2 and 3), we prepared a series of so-called acyl-sulfonamides in which *N*-(methylsulfonyl)carbamoyl or *N*-(*N*,*N*-dime-thylsulfonyl)carbamoyl substituents were introduced at the RHS (types Ib-c and IIb-c, Figs. 2 and 3). In the acylsulfonamide series, the pre-dicted pKa of the sulfonamide nitrogen is lower (pKa ~4.2, Marvin-Sketch from Chemaxon Ltd) than for *N*-(thiazol-2-yl)sulphonamides (pKa ~5.6, MarvinSketch from Chemaxon Ltd), and the compounds also have lower lipophilicity and volume. For the type Ic compounds, benzofuran-2-yl and 4-chlorophenoxyeth-1-yl substituents were intro-duced into the LHS, inspired by some of the most promising hits ob-tained in the similarity search (**TSS-34**, **TSS-42**, Table 3).

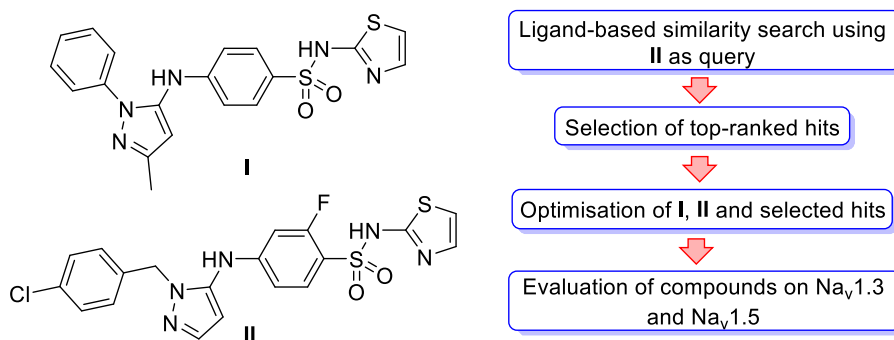The compound **III** was recently shown by our group to be a potent

Fig. 1. General design strategy for new aryl- and acylsulfonamide inhibitors based on Na$_v$1.3 inhibitors **I** and **II**. Similarity search was performed on a drug-like subset of the ZINC library of compounds using ROCS and EON from OpenEye Scientific Software, Inc., and compound **II** as a query [42,43].
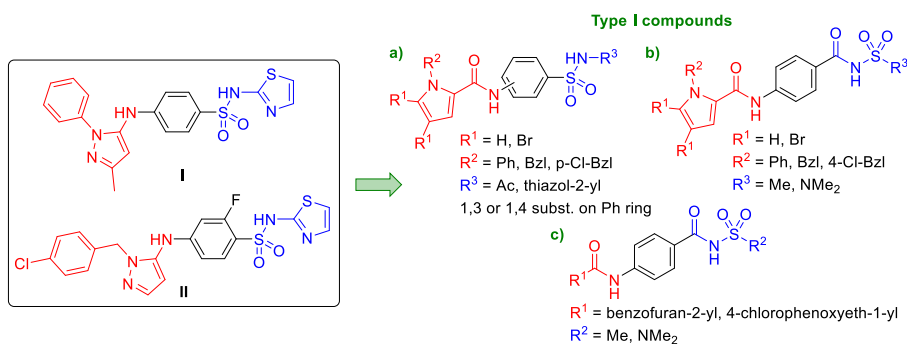

Fig. 2. Proposed structural modifications of Na$_v$1.3 inhibitors **I** and **II** for the design of improved aryl- and acylsulfonamide Na$_v$1.3 inhibitors (type I compounds).
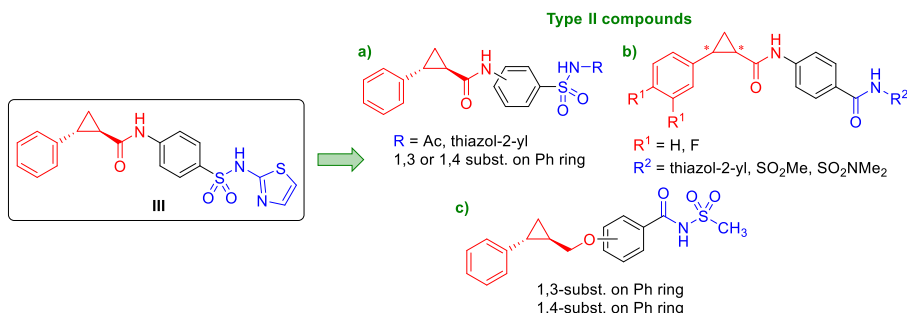

Fig. 3. Proposed structural modifications of Na$_v$1.3 inhibitor **III** [46] for the design of improved aryl- and acylsulfonamide Na$_v$1.3 inhibitors (type II compounds).

inhibitor of human Na$_v$1.3 with an IC$_{50}$ of 56 nM for the inactivated state of the channel and with good selectivity for other Na$_v$1.x isoforms [45]. We prepared a series of its analogues (Fig. 3) to further investigate the importance of the 2-phenylcyclopropane-1-carboxamide moiety (coloured red, Fig. 3) for biological activity. Both aryl- (type IIa, Fig. 3) and

acylsulfonamide series (types IIb-c, Fig. 3) were prepared. For the type IIc compounds, the 2-phenylcyclopropane group was attached to the central benzene ring via a methyleneoxy group to increase the flexibility of the molecules.

Chemistry. The substituted pyrrole-2-carboxylic acids **3a-e** required

1a (R^1 = H, R^2 = OCH$_3$)
1b (R^1 = H, R^2 = CCl$_3$)
1c (R^1 = Br, R^2 = OCH$_3$)

2a (R^1 = H, R^2 = OCH$_3$, R^3 = Ph)
2b (R^1 = H, R^2 = CCl$_3$, R^3 = Bzl)
2c (R^1 = H, R^2 = CCl$_3$, R^3 = 4-Cl-Bzl)
2d (R^1 = Br, R^2 = OCH$_3$, R^3 = Ph)
2e (R^1 = Br, R^2 = OCH$_3$, R^3 = Bzl)

3a (R^1 = H, R^2 = Ph)
3b (R^1 = H, R^2 = Bzl)
3c (R^1 = H, R^2 = 4-Cl-Bzl)
3d (R^1 = Br, R^2 = Ph)
3e (R^1 = Br, R^2 = Bzl)

Scheme 1. Synthesis of 1*H*-pyrrole-2-carboxylic acids **3a-e**^{a}
^{a}Reagents and conditions: (a) phenylboronic acid, Cu (OAc)$_2$, pyridine, CH$_2$Cl$_2$, 35 °C, 20 h (for the synthesis of **2a** and **2d**); NaH, benzyl bromide or 4-chlorobenzyl chloride, DMF, 0 °C → rt, 1–10 h (for the synthesis of **2b-c** and **2e**); (b) 2 M NaOH, THF, 50 °C, 15 h (for the synthesis of **3a** and **3d-e**); 2 M NaOH, THF, rt, 5 h (for the synthesis of **3b-c**).
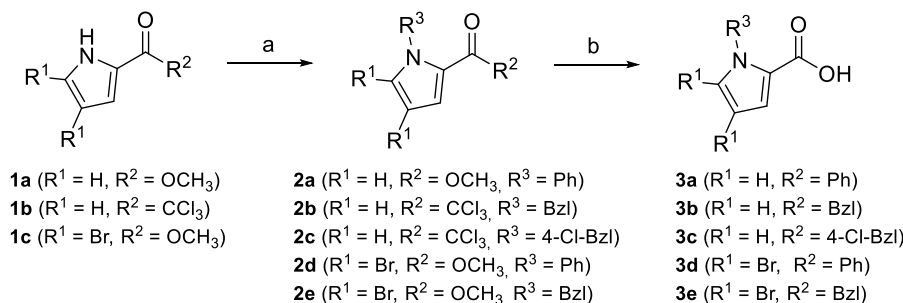
for the synthesis of the type I and type II compounds were first prepared (Scheme 1). In the first step, methyl 1*H*-pyrrole-2-carboxylate (**1a**), 2,2,2-trichloro-1-(1*H*-pyrrol-2-yl)ethan-1-one (**1b**), and methyl 4,5-dibromo-1*H*-pyrrole-2-carboxylate (**1c**) were *N*-substituted with phenyl, benzyl, or 4-chlorobenzyl groups (**2a-e**). The phenyl substituents were introduced with phenylboronic acid, copper(II) acetate and pyridine, while the benzyl and 4-chlorobenzyl groups were introduced with sodium hydride and benzyl bromide or 4-chlorobenzyl chloride as reagents. Alkaline hydrolysis of the trichloromethyl ketone or methyl ester groups of **2a-e** gave the pyrrole-2-carboxylic acids **3a-e**.

Amines **6a** and **10** were prepared according to Schemes 2 and 3, respectively. For the preparation of compound **6a**, the 3-nitrobenzenesulfonyl chloride (**4**) was first reacted with thiazol-2-amine and the resulting compound **5** was then catalytically hydrogenated to give the amine **6a**. To prepare *N*-((4-aminophenyl)sulfonyl)acetamide (**10**), 4-nitrobenzenesulfonamide (**8**) was *N*-acetylated with acetic anhydride and zinc(II) chloride, and then the nitro group of **9** was reduced to the amino group.

Scheme 4 summarises the synthetic procedure for the preparation of aryl- and acylsulfonamides **12a-e**, **13**, **14a-i** and **15a-b** by coupling of carboxylic acids **3a-e**, (1*R*,2*R*)-2-phenylcyclopropane-1-carboxylic acid (**11a**) or 2-(3,4-difluorophenyl)cyclopropane-1-carboxylic acid (**11b**) with amines **6a**, 4-amino-*N*-(thiazol-2-yl)benzenesulfonamide (**6b**) or **10**. Compounds **13** an **14d** were prepared by TBTU-promoted coupling with *N*-methylmorpholine as base and *N,N*-dimethylformamide as solvent. Since the reaction yields of the TBTU-promoted coupling were low, for the rest of the series, pyrrole-2-carboxylic acids **3a-e** or 2-phenylcyclopropane-1-carboxylic acids **11a-b** were first activated with oxalyl chloride in the form of acid chlorides, and then reacted with the corresponding amines **6a-b** or **10** to give the target compounds **12a-e**, **14a-c**, **14e-i** and **15a**.

Compound **19**, the carboxamide analogue of compound **III**, was synthesized according to Scheme 5. First, 4-nitro-*N*-(thiazol-2-yl)benzamide (**17**) was prepared by reacting 4-nitrobenzoyl chloride (**16**) with thiazol-2-amine. The nitro group of compound **17** was then reduced, and the resulting amine **18** was coupled with (1*R*,2*R*)-2-phenylcyclopropane-1-carboxylic acid (**11a**) using oxalyl chloride as reagent to give compound **19**.

For the synthesis of 4-amino-*N*-(sulfamoyl)benzamides **23a** and **23b** (Scheme 6), methanesulfonamide (**21a**) and *N,N*-dimethylsulfamide (**21b**) were first prepared by the reaction of methanesulfonyl chloride (**20a**) or dimethylsulfamoyl chloride (**20b**) with ammonia. In the next step, a proton from the NH$_2$ group of **21a** or **21b** was removed with sodium hydride, the obtained *N*-nucleophile was reacted with 4-nitrobenzoyl chloride (**16**). Finally, the nitro groups of **22a-b** were reduced by catalytic hydrogenation.

To prepare 2-(4-chlorophenoxy)propanoic acids **27a-b**, a Mitsunobu reaction was first carried out between 4-chlorophenol (**24**) and the (*S*)- or (*R*)-isomer of the lactic acid methyl ester (**25a-b**) to give compounds **26a-b**, followed by hydrolysis of the methyl ester groups under aqueous alkaline conditions (Scheme 7).

The synthesis of acyl sulfonamides **29a-d**, **30**, **31a-c** and **32a-c** is presented in Scheme 8. First, carboxylic acids **3a-c**, **11a-b**, **27a-b** or benzofuran-2-carboxylic acid (**28**) were activated with oxalyl chloride, and then, to obtain final products, reacted with corresponding amines **23a** or **23b** in a mixture of dichloromethane and pyridine.

More flexible analogues of the 4-amino-*N*-(sulfamoyl)benzamide
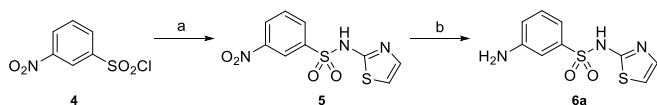
31a, compounds **36a** and **36b**, were synthesized according to Scheme 9. The carbonyl group of **11a** was first reduced with lithium aluminium hydride, and then the resulting alcohol **33** was reacted with methyl 3- or 4-hydroxybenzoate in a Mitsunobu reaction. Compounds **34a** and **34b** were subjected to alkaline hydrolysis, and the resulting carboxylic acids **35a** and **35b** were activated with oxalyl chloride in the form of acid chlorides and then reacted with methanesulfonamide (**21a**), which was pretreated with sodium hydride to remove a proton from the amino group.

Inhibitory activity on Na$_v$1.3 and Na$_v$1.5 channels. All 31 synthesized compounds and 16 compounds identified by a 3D ligand-based similarity search were evaluated for their inhibitory effect on the human Na$_v$1.3 channel and for their selectivity toward the cardiac Na$_v$1.5 channel. Channels were expressed in Chinese hamster ovary cells (CHO), and screening was performed with an automated patch clamp electrophysiology assay on the Sophion QPatch HT system (Sophion Bioscience A/S), as described in the Experimental section. IC$_{50}$ values are reported in Tables 1–3 and represent the concentrations of the compound that inhibit a sodium channel current by 50%. Tetrodotoxin and amitriptyline were used as positive controls.
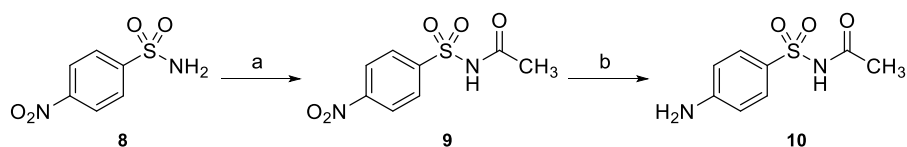
The electrophysiology experiments on Na$_v$1.3 channels were designed to reflect both the resting (closed) state and the inactivated state of the channel. The inactivated state is often the preferred state for pharmacological intervention because under pathophysiological conditions the firing frequency is often higher, resulting in a higher percentage of channels in this functional state. To evaluate the effect of the compounds on the resting state of the channel, a 20-ms activating step to −20 mV was applied starting from a holding potential of −100 mV (Peak 1, Tables 1–3). To evaluate the block of the inactivated state of the channel, the second activating pulse was applied after a 5-s prepulse to half inactivation potential (Peak 2, Tables 1–3). Based on the block of the resting state and the inactivated state, the state selectivity was calculated by comparing the IC$_{50}$ values at Peak1 and Peak 2.

The block of the Na$_v$1.5 channel isoform is associated with an increased risk of cardiac adverse events. Voltage protocols reflecting its physiological cardiac sinus rhythm frequency state were developed for this channel. A pulse train consisting of 10 repetitive activating test pulses was applied at a frequency of 1 Hz. Peak inward currents were determined from the first (Pulse 1) and the tenth (Pulse 10) pulse of each recorded pulse train (Tables 1–3).

Of the 47 compounds tested, eight had IC$_{50}$ values for the Na$_v$1.3 channel in the submicromolar concentration range, and one (**15b**) showed IC$_{50}$ values in the nanomolar range (20 nM). All active compounds acted as state-dependent modulators of the Na$_v$1.3 channel, preferentially blocking the inactivated state of the channels and showing lower activity in the closed state of the channels. The selectivity index between the closed and inactivated states was about one hundred for the most promising inhibitors and about three hundred for the most potent compound **15b**. None of the compounds inhibited the Na$_v$1.5 channel at a concentration of 30 μM. The structure-activity relationships of the compounds for inhibition of Na$_v$1.3 are described below.

Table 2 shows the inhibitory activity of compounds **12a-e**, **13**, **14a-i**, **15a-b**, and **19**. Compounds **14a-i** and **15a-b**, with a thiazol-2-yl substituent attached to the sulfonamide nitrogen at the RHS, were about 20- to 60-fold more effective than compounds **12a-e** and **13** with an acetate group at that position (Scheme 4). This is evident when comparing thiazol-2-yl derivatives **14b** (IC$_{50}$; 1.3 μM), **14d** (IC$_{50}$; 0.38 μM), **14f** (IC$_{50}$; 0.38 μM), **14g** (IC$_{50}$; 0.44 μM), **14i** (IC$_{50}$; 0.33 μM), and **III** (IC$_{50}$; 0.056 μM), with their acetate analogues **12a** (IC$_{50}$; 22 μM), **12b** (IC$_{50}$; 23 μM), **12c** (IC$_{50}$; 7.7 μM), **12d** (IC$_{50}$; 19 μM), **12e** (IC$_{50}$; 7.4 μM), and **13** (IC$_{50}$; 2.0 μM).

When concentrated on the LHS, compounds with a benzyl group attached to the pyrrole nitrogen were generally more effective than compounds with a phenyl group at that position. For example, benzyl-containing compounds **12e** (IC$_{50}$; 7.4 μM), **14c** (IC$_{50}$; 2.9 μM), and **14d** (IC$_{50}$; 0.38 μM) were more active than their corresponding phenyl

Scheme 2. Synthesis of 3-amino-*N*-(thiazol-2-yl)benzenesulfonamide (**6a**)[a]
[a]Reagents and conditions: (a) thiazol-2-amine, Et$_3$N, 4-DMAP, CH$_2$Cl$_2$, rt, 5 h; (b) H$_2$, Pd–C, MeOH/THF (1/2), rt, 15 h.

Scheme 3. Synthesis of *N*-((4-aminophenyl)sulfonyl)acetamide (**10**)[a]
[a]Reagents and conditions: (a) Ac₂O, ZnCl₂, rt, 2 h; (b) H₂, Pd–C, EtOH/THF (1/1), rt, 15 h.
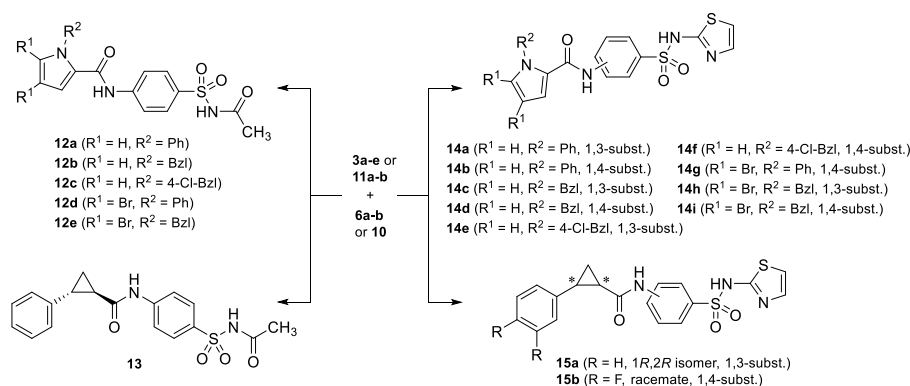
Scheme 4. Synthesis of aryl and acylsulfonamides **12a-e**, **13**, **14a-i** and **15a-b** [a]
[a]Reagents and conditions: (*i*) **3a-e** or **11a-b**, oxalyl chloride, CH₂Cl₂, rt, 15 h, (*ii*) **6a-b** or **10**, CH₂Cl₂, pyridine, rt, 15 h (for the synthesis of **12a-e**, **14a-c**, **14e-i**, **15a-b**); **3b** or **11a**, **6b** or **10**, TBTU, NMM, DMF, 50 °C, 15 h (for the synthesis of **13** and **14d**).
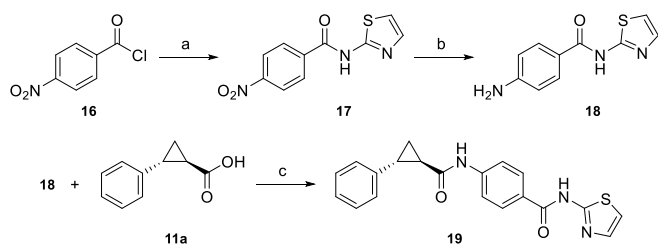

Scheme 5. Synthesis of 4-((1*R*,2*R*)-2-phenylcyclopropane-1-carboxamido)-*N*-(thiazol-2-yl)benzamide (**19**)[a]
[a]Reagents and conditions: (a) pyridine, 1,2-dichloroethane, 60 °C, 15 h; (b) H₂, Pd–C, AcOH/EtOH/THF, rt, 15 h; (c) (*i*) **11a**, oxalyl chloride, CH₂Cl₂, rt, 15 h, (*ii*) **18**, CH₂Cl₂, pyridine, rt, 5 h.

analogues **12d** (IC₅₀; 19 μM), **14a** (IC₅₀; >30 μM), and **14b** (IC₅₀; 1.3 μM).

Introduction of bromine substituents on the pyrrole group or chlorine substituents on the benzyl group increased the activity at Na$_v$1.3 in most cases. The largest increase was observed when comparing the unsubstituted compound **12b** (IC₅₀; 23 μM) with its chlorinated (**12c**, IC₅₀; 7.7 μM) or brominated (**12e**, IC₅₀; 7.4 μM) analogue, and when comparing the unsubstituted compound **14b** (IC₅₀; 1.3 μM) with its brominated analogue **14g** (IC₅₀; 0.44 μM).

Compounds with the 1,4-disubstitution pattern on the central benzene ring were about 10 times more potent than their analogues with the 1,3-disubstitution pattern. This is evident when comparing **14a** (IC₅₀; >30 μM) with **14b** (IC₅₀; 1.3 μM), **14c** (IC₅₀; 2.9 μM) with **14d** (IC₅₀; 0.38 μM), **14e** (IC₅₀; 4.8 μM) with **14f** (IC₅₀; 0.38 μM), **14h** (IC₅₀; 3.5 μM) with **14i** (IC₅₀; 0.33 μM), and **15a** (IC₅₀; 5.1 μM) with compound **III** (IC₅₀; 0.056 μM).
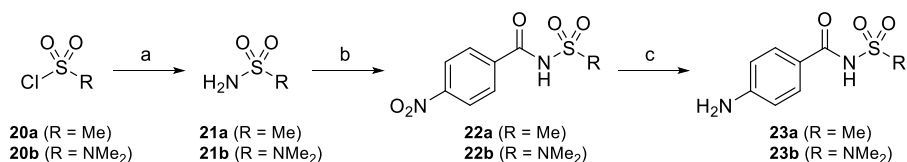
Scheme 6. Synthesis of 4-amino-*N*-(sulfamoyl)benzamides **23a** and **23b**[a]
[a]Reagents and conditions: (a) NH₃₍g₎, THF, rt, 30 min (for the synthesis of **21a**); 7 N NH₃ in MeOH, 60 °C, 15 h (for the synthesis of **21b**); (b) (*i*) NaH, THF, 0 °C, 30 min (*ii*) **16**, 50 °C, 15 h; (c) H₂, Pd–C, AcOH/EtOH, rt, 15 h.
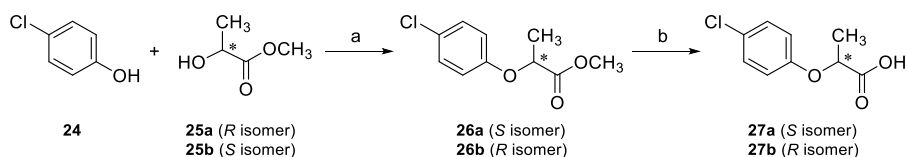
Scheme 7. Synthesis of 2-(4-chlorophenoxy)propanoic acids **27a-b**[a]
[a]Reagents and conditions: (a) Ph₃P, DIAD, CH₂Cl₂, rt, 15 h; (b) 2 M LiOH, MeOH/H₂O (5/1), rt, 5 h.
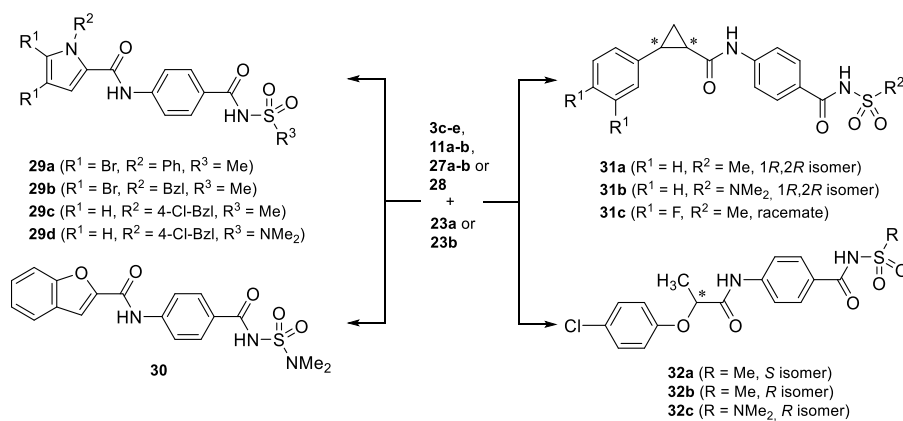
Scheme 8. Synthesis of acyl sulfonamides **29a-d**, **30**, **31a-c** and **32a-c**[a]
[a]Reagents and conditions: (*i*) **3a-c**, **11a-b**, **27a-b** or **28**, oxalyl chloride, CH_2Cl_2, rt, 15 h, (*ii*) **23a** or **23b**, CH_2Cl_2, pyridine, rt, 5 h.
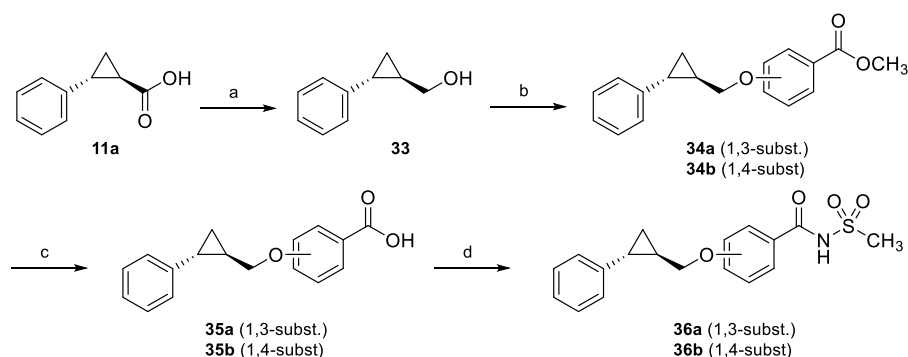

Scheme 9. Synthesis of acyl sulfonamides **36a** and **36b**[a]
[a]Reagents and conditions: (a) $LiAlH_4$, THF, 0 °C, 5 h; (b) methyl hydroxybenzoate, Ph_3P, DIAD, THF, 50 °C, 15 h; (c) 2 M LiOH, MeOH/H_2O, rt, 15 h; (d) (*i*) oxalyl chloride, CH_2Cl_2, rt, 5 h, (*ii*) methanesulfonamide, NaH, THF, 50 °C, 15 h.

The most active compound in the series was **15b** (IC_{50}; 0.020 μM) with a 2-(3,4-difluorophenyl)cyclopropane-1-carboxamide group at the LHS. The two fluorine substituents on the LHS phenyl ring slightly increased the activity compared with compound **III** (IC_{50}; 0.056 μM). The 1,4-disubstitution pattern on the central benzene ring in compound **III** was significantly more optimal than the 1,3-disubstitution pattern in compound **15a** (IC_{50}; 5.1 μM). Finally, replacement of the RHS sulfonamide bond in compound **III** with the amide bond in compound **19** (IC_{50}; 0.99 μM) resulted in twofold lower activity.

Fig. 4 shows the example current traces of the resting-state (P1) and inactivated-state (P2) current for $Na_v1.3$ in the presence of **15b**, DMSO and TTX (Fig. 4a), an overview of the voltage protocol diagram (Fig. 4b), and a concentration-response curve of the effects of **15b** on the amplitude of the sodium currents observed during P1 and P2 (Fig. 4c).

Table 2 shows the inhibitory activities of the prepared acyl sulfonamides **29a-d**, **30**, **31a-c**, **32a-c**, and **36a-b** in which *N*-(methylsulfonyl) carbamoyl or *N*-(*N,N*-dimethylsulfonyl)carbamoyl substituents were introduced at the RHS. Interestingly, this modification completely abolished the activity of the compounds at $Na_v1.3$ channels, as none of the prepared derivatives showed inhibitory activity at concentrations lower than 30 μM.
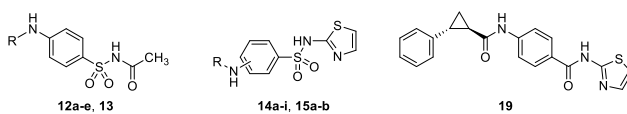
Table 3 shows the inhibitory activity of the compounds selected by a 3D ligand-based similarity search using $Na_v1.3$ inhibitor **II** (Fig. 1) as query. ZINC database was first screened using ROCS similarity searching software. Compounds in the hitlist were ranked according to the TanimotoCombo score, which is a sum of ShapeTanimoto and ColorTanimoto scores. In general, the highest ranked compounds had higher ShapeTanimoto than ColorTanimoto similarities. Therefore, ROCS hitlist was used further in EON similarity searching, which, in addition to the shape similarity, calculated the electrostatic similarities between the pre-aligned query molecule and compounds from the ROCS hitlist. This ligand-based virtual screening methodology resulted in a library of potential $Na_v1.3$ inhibitors similar in shape and electrostatic properties to inhibitor **II**. Sixteen of virtual hits were purchased and tested for $Na_v1.3$ inhibition (Table 3). The strongest inhibitors in the series were **TSS-34** (IC_{50}; 0.32 μM) and **TSS-42** (IC_{50}; 0.24 μM), both containing the *N*-(thiazol-2-yl)sulfonamide moiety at the RHS. These two compounds showed a state selectivity index of about one hundred and did not inhibit $Na_v1.5$ at 30 μM. Both **TSS-34** and **TSS-42** have a 1,4-disubstitution pattern on the central benzene ring and a hydrophobic group on the LHS, containing a chloro substituent attached to the aromatic ring. The third most potent compound from 3D similarity searching, **TSS-39** (IC_{50}; 3.8 μM), also contains an *N*-(thiazol-2-yl)sulfonamide moiety at the RHS, suggesting that this structural feature is optimised for binding to VSD4 and for making contacts with the fourth arginine of the S4 helix. Replacement of the thiazol-2-yl substituent with other aromatic groups, e.g., 5-methylisoxazol-3-yl (**TSS-37**, IC_{50}; >30 μM), phenyl (**TSS-41**, IC_{50}; >30 μM), 2,6-dimethylphenyl (**TSS-42**, IC_{50}; >30 μM) and 3,4-dimethylisoxazol-5-yl (**TSS-48**, IC_{50}; >30 μM), or aliphatic groups, e. g., acyl (**TSS-35**, **TSS-36**, and **TSS-46**, IC_{50}; >30, 21, and 15 μM, respectively) and pyrrolidin-1-yl (**TSS-40**, IC_{50}; 20 μM), resulted in lower $Na_v1.3$ inhibitory activity.

The binding modes of the most potent $Na_v1.3$ inhibitors in our series, **14i**, **15b** and **TSS-42**, were investigated by molecular docking (Fig. 5). The recently published cryo-EM structure of $Na_v1.3$ in complex with the inhibitor ICA121431 (PDB entry 7W7F) [16] bound to the VSD of DIV

Table 1

Inhibitory activities of compounds **12a-e, 13, 14a-i, 15a-b** and **19** on human $Na_v1.3$ channels (state-dependent inhibition) and $Na_v1.5$ channels (use-dependent inhibition) expressed in CHO cells determined using the QPatch.

Comp.	R	Subst. on the phenyl ring	$Na_v1.3$			N^e	$Na_v1.5$		N
			Peak 1[a]	Peak 2[b]	State Selectivity (Peak 1/Peak 2) IC_{50} ratio[d]		Pulse 1[f]	Pulse 10[g]	
			IC_{50} (µM)[c]	IC_{50} (µM)			IC_{50} (µM)	IC_{50} (µM)	
12a		–	>30	22 ± 10	1.4	4	n.d.[h]	n.d.	n.d.
12b		–	>30	23 ± 12	1.3	3	n.d.	n.d.	n.d.
12c		–	>30	7.7 ± 3.5	3.9	3	n.d.	n.d.	n.d.
12d		–	>30	19 ± 10	1.6	3	n.d.	n.d.	n.d.
12e		–	>30	7.4 ± 1.9	4.1	3	n.d.	n.d.	n.d.
13		–	>30	2.0 ± 0.7	15	3	>30	>30	6
14a		1,3	>30	>30	1.0	3	n.d.	n.d.	n.d.
14b		1,4	>30	1.3 ± 0.3	23	4	>30	>30	3
14c		1,3	>30	2.9 ± 1.3	10	4	>30	>30	3
14d		1,4	>30	0.38 ± 0.09	79	4	>30	>30	5
14e		1,3	>30	4.8 ± 2.1	6.2	5	>30	>30	6
14f		1,4	27 ± 6	0.38 ± 0.11	70	3	>30	>30	4
14g		1,4	>30	0.44 ± 0.02	68	3	>30	>30	3

(continued on next page)

Table 1 (*continued*)

Comp.	R	Subst. on the phenyl ring	Na$_v$1.3			N^e	Na$_v$1.5		N
			Peak 1^a	Peak 2^b	State Selectivity (Peak 1/Peak 2) IC$_{50}$ ratio^d		Pulse 1^f	Pulse 10^g	
			IC$_{50}$ (μM)^c	IC$_{50}$ (μM)			IC$_{50}$ (μM)	IC$_{50}$ (μM)	
14h		1,3	24 ± 10	3.5 ± 1.9	7.0	4	>30	>30	4
14i		1,4	27 ± 6	0.33 ± 0.08	82	4	>30	>30	4
15a		1,3	>30	5.1 ± 1.3	5.9	4	>30	>30	3
15b		1,4	6.9 ± 3.6	0.020 ± 0.010	340	5	>30	>30	3
19	–	–	17 ± 8	0.99 ± 0.39	17	6	>30	>30	
TTX^i	–	–	0.0043 ± 0.0009	0.0015 ± 0.0002	2.9	4	n.d.	n.d.	n.d.
AMT^j	–	–	n.d.	n.d.	n.d.	n.d.	11 ± 4	6.9 ± 2.3	5

^{a} Resting-state Na$_v$1.3 current.
^{b} Inactivated-state Na$_v$1.3 current.
^{c} Concentration of compound that inhibits the channel current by 50%.
^{d} Ratio between resting- and inactivated-state IC$_{50}$ values – a measure of state-dependent inhibition of Na$_v$1.3.
^{e} Number of independent experiments.
^{f} Na$_v$1.5 tonic 1 Hz pulse 1 QPatch potency.
^{g} Na$_v$1.5 phasic pulse 10 QPatch potency.
^{h} Not determined.
^{i} Tetrodotoxin.
^{j} Amitriptyline.

was used for docking calculations using the Glide XP protocol (Schrödinger LLC). The *N*-(thiazol-2-yl)sulfonamide moiety was placed in the same binding conformation and orientation as in the case of inhibitor ICA121431. In the binding pocket, it formed ionic interactions with the Arg1627 and Arg1630 side chains, while additional hydrogen bonds were formed between the thiazole nitrogen atom and the Arg1630 guanidinium group, and the sulfonamide oxygen atom and the Asn1562 side chain. In addition, there were also hydrophobic contacts with Ala1626. This interaction network is the key determinant for the potency of the inhibitors. The 1,4-substituted phenyl ring formed hydrophobic contacts with Met1604, while the additional lipophilic substituent of **14i**, **15b** and **TSS-42** stabilized the binding conformation of the inhibitor by interacting with Leu1563 and Phe1605.

Inhibitory activity on other Na$_v$ isoforms. For the selected most promising inhibitors of Na$_v$1.3 (**14f**, **14g**, **14i**, **15b** and **19**), activities on Na$_v$1.7 channels were assessed using an automated patch clamp assay. Channels were expressed in CHO cells, and the assay was performed as described in Experimental section. The results are shown in Table 4. The compounds showed state-dependent activity as there was an enhanced level of block for the inactivated state of the channels and reduced potency against the closed state of the channel. Compounds **14f**, **14g**, **14i** and **15b** had IC$_{50}$ values between 7 and 9 μM, while compound **19** was inactive up to 30 μM. Overall, activity on Na$_v$1.7 was about 20 times lower for compounds **14f**, **14g**, and **14i** than on Na$_v$1.3 and about 350 times lower for the strongest compound **15b**. To investigate the state-dependent effects of selected compounds on Na$_v$1.5 channels, we performed a similar experimental protocol as for Na$_v$1.3 and Na$_v$1.7 channels. The results are shown in Table 4. The compounds showed state-dependent activity on Na$_v$1.5 by inhibiting only the inactivated state of the channel and exerting no activity on the resting state up to 30

μM. For compounds **14f**, **14g**, **14i** and **15b**, the IC$_{50}$ values measured in the inactivated state ranged from 3 to 4 μM. For compounds **14f**, **14g** and **14i**, the activity on Na$_v$1.5 was about 10 times lower than on Na$_v$1.3, and for the most active compound **15b**, the activity was 150 times lower.

To further investigate the Na$_v$1.x selectivity, for the most promising inhibitors of the Na$_v$1.3 channels with IC$_{50}$ values below 10 μM (**12c**, **12e**, **13**, **14b-i**, **15a-b**, **19**, **TSS-34**, **TSS-39**, **TSS-42**), and for some other selected compounds (**29a-d**, **30**, **31a-c**, **32a-c**, **36a-b**, **TSS-33**), the inhibitory activities on the closed state of the Na$_v$1.1, Na$_v$1.2, Na$_v$1.3, Na$_v$1.4, Na$_v$1.5, Na$_v$1.6, Na$_v$1.7, and Na$_v$1.8 channel isoforms were determined (Supplementary information, Table 2S). For these experiments, Na$_v$ channels were expressed in *Xenopus laevis* oocytes, and the two-electrode voltage-clamp method was used for electrophysiology experiments. All compounds were tested at a concentration of 1 μM against the closed state of the sodium channels, and at this concentration, none of the compounds displayed any activity against the Na$_v$1.1-Na$_v$1.2 or Na$_v$1.4-Na$_v$1.8 channel isoforms. The same two-electrode voltage-clamp method was used to determine the activity of selected compounds (**14d**, **14f**, **14g**, **14i**, **15b**, **TSS-34**, **TSS-42**) also against the closed state of the Na$_v$1.3 channel (Supplementary information, Table 2S). Representative whole-cell current traces in the presence of compound **15b**, the voltage protocol used for the experiments, and the bar graph showing the percent inhibition of Na$_v$1.3, Na$_v$1.6, and Na$_v$1.7 current by 1 μM **15b** are shown in Fig. 1S (Supplementary information). The most potent compound in the series was compound **15b** with a moderate 9% blockade of the resting-state current at 1 μM. However, since we have already shown that the compounds act by blocking the inactivated state of the channels, we decided to also evaluate the state-dependent effects. To determine state-dependent inhibition, the
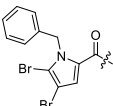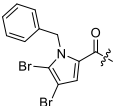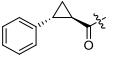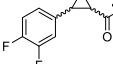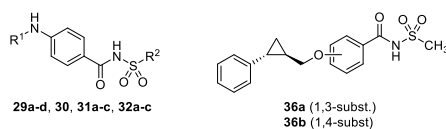
Table 2

Inhibitory activities of compounds **29a-d**, **30**, **31a-c**, **32a-c** and **36a-b** on human $Na_v1.3$ channels (state-dependent inhibition) and $Na_v1.5$ channels (use-dependent inhibition) expressed in CHO cells determined using the QPatch.

29a-d, 30, 31a-c, 32a-c

36a (1,3-subst.)
36b (1,4-subst)

Comp.	R^1	R^2	$Na_v1.3$			N^e	$Na_v1.5$		N
			Peak 1[a]	Peak 2[b]	State Selectivity (Peak 1/Peak 2) IC_{50} ratio[d]		Pulse 1[f]	Pulse 10[g]	
			IC_{50} (µM)[c]	IC_{50} (µM)			IC_{50} (µM)	IC_{50} (µM)	
29a		CH_3	>30	>30	1.0	4	n.d.[h]	n.d.	n.d.
29b		CH_3	>30	>30	1.0	4	n.d.	n.d.	n.d.
29c		CH_3	>30	>30	1.0	4	n.d.	n.d.	n.d.
29d		$N(CH_3)_2$	>30	>30	1.0	4	n.d.	n.d.	n.d.
30		$N(CH_3)_2$	>30	>30	1.0	4	n.d.	n.d.	n.d.
31a		CH_3	>30	>30	1.0	4	n.d.	n.d.	n.d.
31b		$N(CH_3)_2$	>30	>30	1.0	4	n.d.	n.d.	n.d.
31c		CH_3	>30	>30	1.0	4	n.d.	n.d.	n.d.
32a		CH_3	>30	>30	1.0	4	n.d.	n.d.	n.d.
32b		CH_3	>30	>30	1.0	4	n.d.	n.d.	n.d.
32c		$N(CH_3)_2$	>30	>30	1.0	4	n.d.	n.d.	n.d.
36a	–	–	>30	2.1 ± 1.9	14	6	>30	>30	3
36b	-	-	>30	2.3 ± 1.3	13	5	>30	>30	3
TTX[i]	-	–	0.0043 ± 0.0009	0.0015 ± 0.0002	2.9	4	n.d.	n.d.	n.d.
AMT[j]	-	–	n.d.	n.d.	n.d.	n.d.	11 ± 4	6.9 ± 2.3	3

[a] Resting-state $Na_v1.3$ current.

[b] Inactivated-state $Na_v1.3$ current.

[c] Concentration of compound that inhibits the channel current by 50%.

[d] Ratio between resting- and inactivated-state IC_{50} values – a measure of state-dependent inhibition of $Na_v1.3$.

[e] Number of independent experiments.

[f] $Na_v1.5$ tonic 1 Hz pulse 1 QPatch potency.

[g] $Na_v1.5$ phasic pulse 10 QPatch potency.

[h] Not determined.
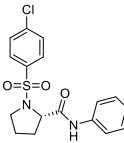
[i] Tetrodotoxin.

[j] Amitriptyline.

Table 3

Inhibitory activities of compounds identified with similarity search on human $Na_v1.3$ channels (state-dependent inhibition) and $Na_v1.5$ channels (use-dependent inhibition) expressed in CHO cells determined using the QPatch.

Comp.	Structure	$Na_v1.3$			N^e	$Na_v1.5$		N
		Peak 1[a]	Peak 2[b]	State Selectivity (Peak 1/Peak 2) IC_{50} ratio[d]		Pulse 1[f]	Pulse 10[g]	
		IC_{50} (µM)[c]	IC_{50} (µM)			IC_{50} (µM)	IC_{50} (µM)	
TSS-33		>30	12 ± 12	2.6	4	n.d.[h]	n.d.	n.d.
TSS-34		>30	0.32 ± 0.25	94	4	>30	>30	4
TSS-35		>30	>30	1.0	4	n.d.	n.d.	n.d.
TSS-36		>30	21 ± 8	1.4	3	n.d.	n.d.	n.d.
TSS-37		>30	>30	30	3	n.d.	n.d.	n.d.
TSS-38		>30	>30	1.0	3	n.d.	n.d.	n.d.
TSS-39		26 ± 8	3.8 ± 1.9	7.0	4	>30	>30	3
TSS-40		>30	20 ± 9	1.5	3	n.d.	n.d.	n.d.
TSS-41		>30	>30	1.0	3	n.d.	n.d.	n.d.
TSS-42		>30	0.24 ± 0.07	130	5	>30	>30	3
TSS-43		>30	25 ± 8	1.2	3	n.d.	n.d.	n.d.
TSS-44		>30	28 ± 3	1.1	4	n.d.	n.d.	n.d.
TSS-45		>30	>30	30	3	n.d.	n.d.	n.d.

(*continued on next page*)

Table 3 (*continued*)

Comp.	Structure	Na$_v$1.3			N[e]	Na$_v$1.5		N
		Peak 1[a]	Peak 2[b]	State Selectivity (Peak 1/Peak 2) IC$_{50}$ ratio[d]		Pulse 1[f]	Pulse 10[g]	
		IC$_{50}$ (μM)[c]	IC$_{50}$ (μM)			IC$_{50}$ (μM)	IC$_{50}$ (μM)	
TSS-46		>30	15 ± 7	2.0	3	n.d.	n.d.	n.d.
TSS-47		>30	>30	1.0	3	n.d.	n.d.	n.d.
TSS-48		>30	>30	1.0	4	n.d.	n.d.	n.d.
TTX[i]	-	0.0043 ± 0.0009	0.0015 ± 0.0002	2.9	4	n.d.	n.d.	n.d.
AMT[j]	-	n.d.	n.d.	n.d.	n.d.	11 ± 4	6.9 ± 2.3	5

[a] Resting-state Na$_v$1.3 current.
[b] Inactivated-state Na$_v$1.3 current.
[c] Concentration of compound that inhibits the channel current by 50%.
[d] Ratio between resting- and inactivated-state IC$_{50}$ values – a measure of state-dependent inhibition of Na$_v$1.3.
[e] Number of independent experiments.
[f] Na$_v$1.5 tonic 1 Hz pulse 1 QPatch potency.
[g] Na$_v$1.5 phasic pulse 10 QPatch potency.
[h] Not determined.
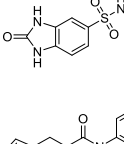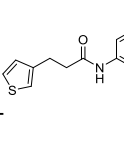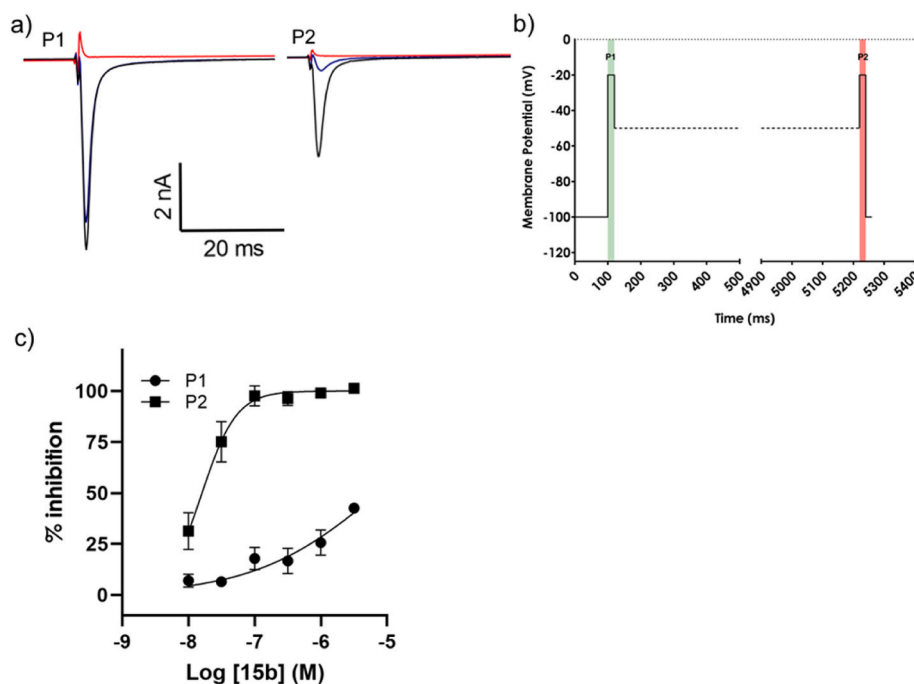[i] Tetrodotoxin.
[j] Amitriptyline.

Fig. 4. Characterization of compound **15b** as an inhibitor of the Na$_v$1.3 channel. Compound **15b** was applied to CHO cells stably expressing the Na$_v$1.3 channel to determine its potency and state dependence. a) Example current traces of resting-state (P1) and inactivated-state current (P2, after a 5-s prepulse to half of the inactivation potential) for a typical recording showing concentration-dependent inhibition of inward currents (black traces = vehicle, blue traces = 300 nM **15b**, red traces = 300 nM TTX). The scale bar shows 2 nA on the y-axis and 20 ms on the x-axis. b) An overview of the voltage protocol diagram. c) A concentration–response curve of the effects of **15b** on the amplitude of sodium currents observed during P1 and P2.

activities of selected compounds (**14d**, **14f**, **14g**, **14i**, **15b**, **TSS-34**, **TSS-42**) at Na$_v$1.3, Na$_v$1.7, and Na$_v$1.8 channels expressed in *Xenopus laevis* oocytes were determined by the two-electrode voltage-clamp method using a standard two-pulse protocol as described for the automated patch-clamp electrophysiology assay (Supplementary information, Table 3S). The compounds showed no activity at Na$_v$1.7 and Na$_v$1.8 channels up to a concentration of 1 μM, confirming their isoform

selectivity. However, the compounds blocked Na$_v$1.3 current in the inactivated state (Peak 2) with 21–63% inhibition at 1 μM. The most active compound was **15b** with a 63% blockade of the inactivated-state current at 1 μM. Since this compound blocked the resting-state current (Peak 1) to a lesser extent (9% block at 1 μM), we confirmed its promising state-dependent activity. Therefore, compounds with low IC$_{50}$ values at Na$_v$1.3 channels (e.g., **14d**, **14f**, **14g**, **14i**, **15b**, **TSS-34**, **TSS-**
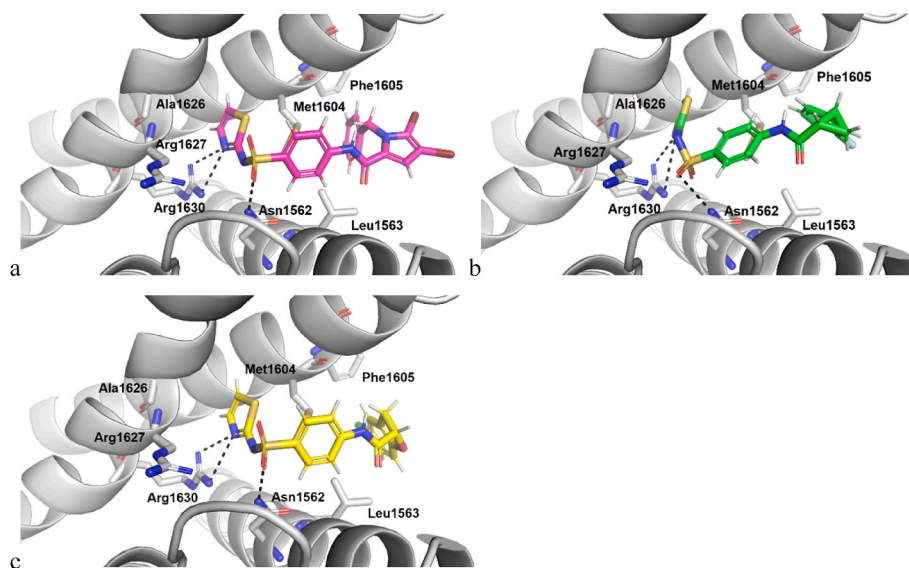
Fig. 5. Binding modes of a) **14i** (in magenta sticks), b) **15b** (in green sticks) and c) **TSS-42** (in yellow sticks) in the Na_v1.3 VSD of DIV (in grey cartoon, PDB entry: 7W7F). For clarity, only amino acids forming hydrogen bonds (black dashed lines), ionic interactions and hydrophobic interactions with inhibitors are shown as sticks.

Table 4
Inhibitory activities of compounds **14f-g**, **14i**, **15b** and **19** on human Na_v1.7 and Na_v1.5 channels (state-dependent inhibition) expressed in CHO cells determined using the QPatch.

Comp.	Na_v1.7				Na_v1.5			
	Peak 1[a]	Peak 2[b]	State Selectivity (Peak 1/Peak 2) IC$_{50}$ ratio[d]	N[e]	Peak 1	Peak 2	State Selectivity (Peak 1/Peak 2) IC$_{50}$ ratio	N
	IC$_{50}$ (μM)[c]	IC$_{50}$ (μM)			IC$_{50}$ (μM)	IC$_{50}$ (μM)		
14f	>30	8.4 ± 3.0	1.4	4	>30	3.7 ± 2.1	2.7	3
14g	>30	9.3 ± 2.1	1.2	4	>30	3.4 ± 1.2	2.9	4
14i	>30	7.1 ± 1.1	1.4	3	>30	3.5 ± 1.7	2.9	5
15b	>30	7.1 ± 3.5	4.3	3	>30	3.0 ± 1.8	3.4	3
19	>30	>30	n.d.[f]	3	>30	>30	n.d.	6
AMT[g]	10 ± 0	2.3 ± 0.8	4.4	7	20 ± 3	1.2 ± 0.4	17	5

[a] Resting-state current.
[b] Inactivated-state current.
[c] Concentration of compound that inhibits the channel current by 50%.
[d] Ratio between resting- and inactivated-state IC$_{50}$ values – a measure of state-dependent inhibition.
[e] Number of independent experiments.
[f] Not determined.
[g] Amitriptyline.

42) can be considered subtype-selective inhibitors of Na_v1.3. However, because of the different expression systems for Na_v1.1, Na_v1.2, Na_v1.3, Na_v1.4, Na_v1.5, Na_v1.6, Na_v1.7, and Na_v1.8 (*Xenopus laevis* oocytes) compared with Na_v1.3 and Na_v1.5 (CHO cells), minor differences in channel function and thus IC$_{50}$ values are expected. The differences may be due to different post-translational modifications or expression of auxiliary subunits that could affect the kinetics of channel gating [47]. In the case of CHO cells, the auxiliary β-subunits were not co-expressed.

Cytotoxicity. The cytotoxic activity of selected Na_v1.3 inhibitors was determined in an MTS (3-(4,5-dimethylthiazol-2-yl)-5-(3-carboxymethoxyphenyl)-2-(4-sulfophenyl)-2*H*-tetrazolium) assay on human HepG2 cells (hepatocellular carcinoma cells). The decrease in cell proliferation after treatment with the compounds was compared with the decrease in cells treated with etoposide at a concentration of 50 μM. None of the compounds showed significant cytotoxic activity at a concentration of 50 μM (Supplementary information, Table 4S).

3. Conclusion

The Na_v1.3 channel is mainly expressed in the CNS of the embryonic brain and has been shown to be upregulated after nerve injury, and mutations in Na_v1.3 are associated with childhood epilepsies and developmental encephalopathies [27,28]. Few selective Na_v1.3 inhibitors are known in the literature, so the discovery of new and potent inhibitors of this channel would allow us to study its role in more detail. Selective Na_v1.3 inhibitors could potentially be used as novel therapeutics to treat pain or neurodevelopmental disorders. In this work, we developed a series of novel Na_v1.3 inhibitors by using known Na_v1.3 inhibitors **I-III** as starting compounds. A total of 31 compounds were synthesized and 16 compounds were selected based on 3D ligand-based similarity search. All active compounds acted as state-dependent inhibitors of Na_v1.3 by inhibiting the inactivated state of the channel and exerting significantly lower activity on the closed form of the channel. Eight compounds had an IC$_{50}$ value of less than 1 μM, and one of the compounds had an IC$_{50}$ value of 20 nM. None of the compounds showed use-dependent inhibition of the cardiac isoform Na_v1.5 at a concentration of 30 μM. Selectivity was also determined for the closed state of Na_v channel isoforms (Na_v1.1-Na_v1.8). Whereas compounds displayed no effect on the closed state of Na_v1.1-Na_v1.2 or Na_v1.4-Na_v1.8 channel isoforms, compound **15b** displayed small, yet selective, effects on the

Na$_v$1.3 channel isoform. In addition, the activities of seven selected compounds on Na$_v$1.3, Na$_v$1.7, and Na$_v$1.8 channels expressed in *Xenopus laevis* oocytes were determined by the two-electrode voltage clamp method with the same two-pulse protocol used to assess Nav1.3 channel activity in the automated patch-clamp experiments. The compounds showed robust effects on the inactivated state of the Na$_v$1.3 channel at 1 μM, but no effect on the inactivated state of the Na$_v$1.7 or Na$_v$1.8 channel, demonstrating that the compounds are selective for the inactivated state of Na$_v$1.3 channel when tested among the Na$_v$1.3, Na$_v$1.7, and Na$_v$1.8 channel isoforms. On the other hand, compounds showed activity on Na$_v$1.3 channels expressed in oocytes, albeit with slightly lower potency compared with the activity observed in patch clamp experiments.

The most important part of the molecule for the good inhibitory effect on Na$_v$1.3 proved to be the *N*-(thiazol-2-yl)sulfonamide moiety at the RHS. At the central benzene ring, the 1,4-disubstitution pattern was most optimal. Various lipophilic groups were tolerated at the LHS, usually containing a terminal aromatic group that could contain halogen substituents. The most potent inhibitor, **15b**, contained a 2-(3,4-difluorophenyl)cyclopropane-1-carboxamide group at the LHS. The activity was also good for the molecules with a benzylated pyrrole ring at this position. Thus, the LHS of the inhibitors seems to be the most suitable part for further optimization. Overall, the Na$_v$1.3 inhibitors we discovered in this work could be used as tools for studying the biological role of this Na$_v$ isoform or for their further development into more potent and selective inhibitors.

4. Experimental section

Electrophysiology. *Automated patch clamp.* The synthesized compounds were evaluated for their inhibitory effects on human voltage-gated sodium channels Na$_v$1.3 and Na$_v$1.5 using the automated patch clamp electrophysiology technique on the Sophion QPatch HT system (Sophion Bioscience A/S). The IC$_{50}$ values of the compounds were calculated from concentration-response curves measured at four relevant concentrations between 0.3 and 10 μM. Cells were detached from T175 cell culture flasks with trypsin-EDTA (0.05%) and stored in serum-free media on board the QPatch HT system. Cells were sampled, washed, and resuspended in extracellular recording solution by the QPatch HT before being added to the wells of the chip. 0.1% DMSO v/v solution was applied to the cells to achieve stable control recording (4 min total), which was completed by applying test sample concentrations (4 min incubation per test concentration). Samples were prepared in extracellular solution with serial dilutions ranging from 10 to 0.3 μM concentration. Measurements on Na$_v$1.3 were performed using a standard two-pulse voltage protocol. Starting from a holding potential of −100 mV, a 20 ms activating step was applied to −20 mV to measure the effect of the compounds on resting-state block. The second activating pulse was applied to the half-inactivation potential after a 5-s prepulse to assess block on the inactivated state of the channel. This protocol was applied with an interval of 0.067 Hz. To measure the Na$_v$1.5 isoform, 10 pulses were applied from −20 mV to a holding potential of −100 mV at 1 Hz. This protocol was applied with an interval of 0.016 Hz for the entire duration of the experiment. Peak inward current measurement of Na$_v$1.3 was performed for both the closed and inactivated test pulses for each sweep and for Na$_v$1.5 from the 10th pulse. Dimethyl sulfoxide (DMSO) was used as a control, and its concentration was kept constant under all conditions. Data were recorded using QPatch assay software (v5.0). Percent peak current inhibition was calculated as the mean peak current value for the last three sweeps measured in each concentration test period relative to the last three sweeps recorded during the vehicle control period. Sigmoidal concentration-response curves were fitted to the inhibition data using Xlfit (IDBS). Data are presented as mean ± standard deviation for at least 3 independent observations.

Two-electrode Voltage Clamp. Expression of voltage-gated ion channels in *Xenopus laevis* oocytes. For the expression of Nav channels, including hNa$_v$1.1, rNa$_v$1.2, rNa$_v$1.3, rNa$_v$1.4, hNa$_v$1.5, mNa$_v$1.6, hNa$_v$1.7, hNa$_v$1.8, together with auxiliary subunits rβ1 and hβ1, in *Xenopus* oocytes, the linearized plasmids were transcribed using the T7 or SP6 mMESSAGE mMACHINE transcription kit (Ambion®, Carlsbad, California, USA). *Xenopus laevis* oocytes at stage V-VI were isolated by partial ovariectomy as previously described [48]. Animals were anesthetized by immersion in 0.1% tricaine methanesulfonate solution (Sigma®) (pH 7.0) for 15 min. The isolated oocytes were defolliculated with 1.5 mg/mL collagenase. Into the defolliculated oocytes, 50 nL of cRNA was injected at a concentration of 1 ng/nL using a microinjector (Drummond Scientific®, Broomall, Pennsylvania, USA). Oocytes were incubated in a solution containing (in mM): NaCl, 96; KCl, 2; CaCl$_2$, 1.8; MgCl$_2$, 2; and HEPES, 5, at a pH of 7.4 supplemented with 50 mg/L gentamycin sulfate. Frogs were used in accordance with license number LA1210239 of the Laboratory of Toxicology and Pharmacology, University of Leuven. All animal care and experimental procedures were in accordance with the guidelines of the "European Convention for the Protection of Vertebrate Animals used for Experimental and other Scientific Purposes" (Strasbourg, 18. III.1986).

Electrophysiological recordings. Two-electrode voltage-clamp recordings were performed at room temperature (18–22 °C) using a Geneclamp 500 amplifier (Molecular Devices®, Downingtown, Pennsylvania, USA) controlled by a pClamp data acquisition system (Axon Instruments®, Union City, California, USA). Whole-cell currents of oocytes were recorded 1–4 days after mRNA injection. The composition of the bath solution was (in mM): NaCl, 96; KCl, 2; CaCl$_2$, 1.8; MgCl$_2$, 2; and HEPES, 5, at pH 7.4. The voltage and current electrodes were filled with 3 M KCl. The resistances of the two electrodes were kept between 0.8 and 1.5 MΩ. The elicited currents were sampled at 20 kHz and filtered at 2 kHz using a four-pole low-pass Bessel filter. Leak subtraction was performed with a -P/4 protocol. For electrophysiological analysis of compounds, a series of protocols were performed at a holding potential of −90 mV. Na$^+$ current traces were elicited by 100 ms depolarizations to Vmax (the voltage corresponding to the maximum Na$^+$ current under control conditions). The effects of the compounds on steady-state inactivation were examined using a standard 2-step protocol. In this protocol, 100-ms conditioning 5-mV step prepulses ranging from −90 to 60 mV were followed by a 50-ms test pulse to −10 mV. Compounds **14d**, **14f**, **14g**, **14i**, **15b**, **TSS -34** and **TSS -42** were also measured on Na$_v$1.3, Na$_v$1.7 and Na$_v$1.8 using a similar standard two-pulse voltage protocol as described for the automated patch clamp experiments. All data are presented as mean ± standard deviation (SD) of at least 5 independent experiments (n ≥ 5). All data were tested for normality with a D'Agustino Pearson omnibus normality test. All data were tested for statistical significance with the Bonferroni test or the Dunn test. Data were analyzed using pClamp Clampfit 10.0 (Molecular Devices®, Downingtown, Pennsylvania, USA) and Origin 7.5 software (Originlab®, Northampton, Massachusetts, USA).

3D similarity searching. A library of drug-like molecules was downloaded from the ZINC database [49]. For these compounds, a library of conformers was generated using the OMEGA software (OMEGA 2.5.1.4: OpenEye Scientific Software, Santa Fe, NM. http://www.eyesopen.com) [50]. Default settings were used to generate the conformers, resulting in a maximum of 200 conformers per ligand.

3D similarity search was first implemented in ROCS (ROCS 3.3.1.2: OpenEye Scientific Software, Santa Fe, NM. http://www.eyesopen.com) [51], using the compound **II** (Fig. 1) as a query. ROCS represents atoms as 3D Gaussian functions [52,53] and calculates similarity as a function of the volume overlaps between alignments of the pre-generated molecular conformers. Chemical ("color") similarity is measured using overlaps between dummy atoms that mark chemical functionalities of interest: Hydrogen bond donors and acceptors, charged functional groups, rings, and hydrophobic groups. The similarity scores for shape (molecular geometry) and color (presence of relevant pharmacophores) are usually combined into a single score (TanimotoCombo) that can be used to rank screening molecules against a query molecule [54]. Ten

thousand highest ranked compounds from the ROCS similarity search were used for virtual screening using EON (EON 2.3.1.2: OpenEye Scientific Software, Santa Fe, NM. http://www.eyesopen.com), which calculates the electrostatic similarity between two compounds in the form of an Electrostatic Tanimoto (ET) score.

Visualization of the hit list of 1000 compounds from EON virtual screening was performed using VIDA software (VIDA 4.3.0.4: OpenEye Scientific Software, Santa Fe, NM. http://www.eyesopen.com). Hits were ranked according to the ET_combo score, which is the sum of the EON ShapeTanimoto and ET_pb scores (Supplementary information, Table 1S). Based on these results, 16 compounds were purchased (Table 3) and tested for $Na_v1.3$ channel inhibition.

Molecular docking. Ligand structures in SMILES format were opened in Maestro (Schrödinger, LLC, New York, NY, USA, 2020). Energy-minimized conformations of compounds **14i**, **15b**, and **TSS-42** were generated with the LigPrep wizard using the OPLS3 force field. The protonation states of the ligands were calculated at pH 7.4 using Epik. Stereoisomers were generated for racemic compounds **15b** and **TSS-42**. Molecular docking calculations were performed using Schrödinger Release 2020–1 (Schrödinger, LLC, New York, NY, USA, 2020). The cryo-EM structure of $Na_v1.3$ in complex with the inhibitor ICA121431 (PDB entry: 7W7F) [16] was retrieved from the Protein Data Bank. The protein was then prepared using the Protein Preparation Wizard with default settings. The receptor grid was calculated for the ligand-binding site, and compounds **14i**, **15b** and **TSS-42** were docked using the Glide XP protocol, as implemented in Schrödinger Release 2020–1 (Glide, Schrödinger, LLC, New York, NY, USA, 2020). The highest scored docking pose of each compound was used for presentation. The figures were created in PyMOL.

***In vitro* cytotoxicity measurements.** Cytotoxicity of selected compounds at a concentration of 50 μM was determined using the MTS assay (Promega Corporation, Madison, WI, USA) according to the manufacturer's instructions. HepG2 cells (ATCC) were cultured in Eagle's MEM medium (Gibco, Thermo Fisher Scientific, Waltham, MA, USA) supplemented with 10% fetal bovine serum (FBS; Gibco, Thermo Fisher Scientific, Waltham, MA, USA), penicillin/streptomycin (100 UI/mL/100 μg/mL; Sigma-Aldrich, St. Louis, MO, USA), and L-glutamine (2 mM; Sigma-Aldrich, St. Louis, MO, USA). Cells were incubated in a humidified atmosphere containing 5% CO_2 at 37 °C. Cells were seeded in 96-well cell culture plates (2000 cells per well in 100 μL growth medium) and incubated for 24 h to allow them to settle in the wells. Cells were then treated with 50 μL of the selected compounds, 50 μM etoposide (positive control; IC_{50} = 20.1 μM [Ref. [55]: 30.2 μM]; TCI, Tokyo, Japan) or 0.5% DMSO (vehicle control) and incubated for 72 h Cell-Titer96® Aqueous One Solution reagent (10 μL; Promega Corporation, Madison, WI, USA) was added to the wells, and the plates were incubated for an additional 3 h. Absorbance at 490 nm was measured using a Synergy H4 microplate reader (BioTek, Winooski, VT, USA). To determine cell viability, the results of wells containing cells treated with the test compound were normalized with the results of cells incubated in 0.5% DMSO. Statistical significance ($p < 0.05$) was calculated using a two-tailed Student's t-test between the treated groups and 0.5% DMSO. Independent experiments were performed in triplicate and repeated twice. Results are expressed as the mean values of the independent measurements.

Chemistry. Chemicals were purchased from Apollo Scientific (Stockport, UK), TCI (Tokyo, Japan), Sigma-Aldrich (St. Louis, USA), and Acros Organics (Geel, Belgium). Thin-layer chromatography (TLC) was performed on Merck 60 F254 silica gel plates (0.25 mm) under visualization with UV light and spray reagents. Column chromatography was performed on silica gel 60 (particle size 240–400 mesh). IR spectra were recorded on a Thermo Nicolet Nexus 470 ESP FT-IR spectrometer (Thermo Fisher Scientific, Waltham, USA). HPLC analyses were performed on an Agilent Technologies 1100 instrument (Agilent Technologies, Santa Clara, USA) with a G1316A thermostat, a G1313A autosampler, and a G1365B UV–Vis detector using a Phenomenex Luna

5-μm C18 column (4.6 × 150 mm or 4.6 × 250 mm, Phenomenex, Torrance, USA) and a flow rate of 1.0 mL/min. The eluent consisted of trifluoroacetic acid (0.1% in water) as solvent A and acetonitrile as solvent B. Melting points were determined using a Reichert hot stage microscope and are uncorrected. ^1H and ^{13}C NMR spectra were recorded at 400 and 100 MHz, respectively, using a Bruker AVANCE III 400 spectrometer (Bruker Corporation, Billerica, USA) in $CDCl_3$ or DMSO-d_6 solutions with TMS as the internal standard. Mass spectra were recorded using a VG Analytical Autospec Q mass spectrometer (Fisons, VG Analytical, Manchester, UK). The purity of the tested compounds was determined to be ≥ 95%.

4.1. Synthetic procedures

4.1.1. General procedure A. Synthesis of compounds 2a and 2d (with 2a as an example)

To a mixture of **1a** (0.500 g, 4.20 mmol) and phenylboronic acid (1.46 g, 12.0 mmol) in anhydrous dichloromethane (10 mL) pyridine (0.970 mL, 12.0 mmol), activated molecular sieves (4 Å) and copper(II) acetate (2.18 g, 12.0 mmol) - prepared from copper(II) acetate monohydrate with drying under vacuum - were added, and the mixture was stirred at rt for 15 h. The obtained suspension was filtered through Celite, the filtrate was concentrated under reduced pressure and purified with flash column chromatography using ethyl acetate/petroleum ether (1:10) as solvent, to obtain **2a** (0.683 g) as white crystals.

4.1.2. Methyl 1-phenyl-1H-pyrrole-2-carboxylate (2a) [56,57]

Synthesized according to General procedure A. White crystals; yield 85% (0.683 g); mp 69–70 °C; ^1H NMR (400 MHz, DMSO-d_6) δ 3.63 (s, 3H, CH_3), 6.32–6.34 (m, 1H, pyrr-H), 7.04–7.06 (m, 1H, pyrr-H), 7.24–7.25 (m, 1H, pyrr-H), 7.33–7.35 (m, 2H, Ar–H), 7.40–7.48 (m, 3H, Ar–H).

4.1.3. General procedure B synthesis of compounds 2b-c and 2e (with 2b as an example)

A solution of compound **1b** (1.00 g, 4.71 mmol) in dry DMF (5 mL) was cooled on an ice bath, sodium hydride (60% dispersion in mineral oil, 207 mg, 5.18 mmol) was added portion wise and the obtained mixture was stirred for 0.5 h. A solution of benzyl bromide (0.560 mL, 4.71 mmol) in DMF (1 mL) was added dropwise and the mixture was stirred at rt for 2 h. Ethyl acetate (50 mL) was added to the solution, the organic phase was washed with water (2 × 20 mL), 10% citric acid (2 × 20 mL) and brine (2 × 15 mL), dried over Na_2SO_4, filtered and evaporated under reduced pressure. The crude product was purified with flash column chromatography using ethyl acetate/petroleum ether (1:10) as solvent, to obtain **2b** (0.973 g) as a brown oil.

4.1.4. 1-(1-Benzyl-1H-pyrrol-2-yl)-2,2,2-trichloroethan-1-one (2b) [58]

Synthesized according to General procedure B. Brown oil; yield 68% (0.973 g); ^1H NMR (400 MHz, $CDCl_3$) δ 5.60 (s, 2H, CH_2), 6.32–6.34 (m, 1H, pyrr-H), 7.09–7.14 (m, 3H, Ar–H), 7.29–7.37 (m, 3H, Ar–H), 7.61–7.63 (m, 1H, pyrr-H).

4.1.5. General procedure C. Synthesis of compounds 3a and 3d-e (with 3a as an example)

Compound **2a** (0.630 g, 3.13 mmol) was dissolved in tetrahydrofuran (10 mL), 2 M NaOH (6.26 mL, 12.5 mmol) was added and the mixture was heated at 50 °C for 15 h. The mixture was neutralized with 1 M HCl and concentrated under reduced pressure, the residual aqueous solution was acidified to pH 2 with 1 M HCl and the product extracted with ethyl acetate (2 × 10 mL). The combined organic phases were washed with 0.1 M HCl (2 × 10 mL) and brine (2 × 10 mL), dried over Na_2SO_4, filtered and the solvent evaporated under reduced pressure to afford **3a** as white solid (533 mg).

4.1.6. 1-Phenyl-1H-pyrrole-2-carboxylic acid (3a) [56]

Synthesized according to General procedure C. White crystals; yield 91% (0.533 g); mp 163–165 °C; ^{1}H NMR (400 MHz, DMSO-d_6) δ 6.28–6.30 (m, 1H, pyrr-H), 6.99–7.00 (m, 1H, pyrr-H), 7.17–7.18 (m, 1H, pyrr-H), 7.32–7.47 (m, 5H, Ar–H), 12.16 (br s, 1H, COOH).

4.1.7. General procedure D. Synthesis of compounds 3b-c (with 3b as an example)

Compound **2b** (0.913 g, 3.02 mmol) was dissolved in tetrahydrofuran (10 mL), 2 M NaOH (4.53 mL, 9.05 mmol) was added and the mixture was stirred at rt for 5 h. The mixture was neutralized with 1 M HCl and concentrated under reduced pressure, the residual aqueous solution was acidified to pH 2 with 1 M HCl and the product extracted with ethyl acetate (2 × 10 mL). The combined organic phases were washed with 0.1 M HCl (2 × 10 mL) and brine (2 × 10 mL), dried over Na$_2$SO$_4$, filtered and the solvent evaporated under reduced pressure to afford **3a** as white crystals (420 mg).

4.1.8. 1-Benzyl-1H-pyrrole-2-carboxylic acid (3b) [59]

Synthesized according to General procedure D. White crystals; yield 69% (420 mg); mp 116–118 °C; ^{1}H NMR (400 MHz, DMSO-d_6) δ 5.56 (s, 2H, CH$_2$), 6.15–6.16 (m, 1H, pyrr-H), 6.86–6.87 (m, 3H, Ar–H), 7.07–7.09 (m, 2H, Ar–H), 7.22–7.33 (m, 4H, Ar–H), 12.16 (br s, 1H, COOH).

4.1.9. 3-Nitro-N-(thiazol-2-yl)benzenesulfonamide (5) [60]

To the solution of 3-nitrobenzenesulfonyl chloride (1.50 g, 6.77 mmol) in dichloromethane (60 mL), thiazol-2-amine (0.847 g, 8.46 mmol), triethylamine (1.18 mL, 8.46 mmol) and 4-DMAP (81 mg, 0.677 mmol) were added and the mixture was stirred at rt for 5 h. Saturated solution of NaHCO$_3$ (60 mL) was added to the mixture, the layers were separated and the organic phase was washed with brine (2 × 30 mL), dried over Na$_2$SO$_4$, filtered and the solvent evaporated under reduced pressure. The residue was purified with flash column chromatography using dichloromethane/methanol (50:1 to 20:1) as solvent, to obtain crude product **5** (0.799 g) as a yellow solid, which was used in the next step without further purification.

4.1.10. 3-Amino-N-(thiazol-2-yl)benzenesulfonamide (6a)

To the solution of compound **5** (0.765 g, 2.68 mmol) in a mixture of tetrahydrofuran (20 mL) and methanol (10 mL) Pd–C (250 mg) was added and the reaction mixture was stirred under hydrogen atmosphere for 48 h. The catalyst was filtered off, the solvent was removed under reduced pressure and the residue was purified with flash column chromatography using dichloromethane/methanol (30:1) as solvent, to obtain product **6a** (162 mg) as a yellow solid. Yield 24% (162 mg); mp 150–153 °C; ^{1}H NMR (400 MHz, DMSO-d_6) δ 5.52 (s, 2H, NH$_2$), 6.69–6.71 (m, 1H, Ar-H-4/6), 6.88 (d, 1H, J = 4.8 Hz, thiazole-H), 6.88–6.90 (m, 1H, Ar-H-4/6), 7.01 (t, 1H, J = 2.0 Hz, Ar-H-2), 7.12 (t, 1H, J = 8.0 Hz, Ar-H-5), 7.24 (d, 1H, J = 4.8 Hz, thiazole-H), 12.63 (br s, 1H, NH).

4.1.11. N-((4-Nitrophenyl)sulfonyl)acetamide (9) [61]

A mixture of 4-nitrobenzenesulfonamide (0.750 g, 3.71 mmol), zinc (II) chloride (50.6 mg, 0.371 mmol) and acetic anhydride (3.16 mL, 33.4 mmol) was stirred at rt for 3 h. Ethyl acetate (20 mL) and water (20 mL) were added to the mixture, the layers were separated and the water phase was extracted with ethyl acetate (20 mL). The combined organic phase was washed with water (2 × 20 mL) and brine (2 × 20 mL), dried over Na$_2$SO$_4$, filtered and the solvent evaporated under reduced pressure. The crude product was recrystallized from toluene, to obtain **9** (0.790 g) as white crystals. Yield 24% (0.790 g); mp 170–173 °C; ^{1}H NMR (400 MHz, DMSO-d_6) δ 1.97 (s, 3H, CH$_3$), 8.17 (d, 1H, J = 8.8 Hz, Ar-H-2,6), 8.45 (d, 1H, J = 8.8 Hz, Ar-H-3,5), 12.46 (br s, 1H, NH).

4.1.12. N-((4-aminophenyl)sulfonyl)acetamide (10)

To the solution of compound **9** (1.01 g, 2.68 mmol) in a mixture of tetrahydrofuran (20 mL) and ethanol (10 mL) Pd–C (300 mg) was added and the reaction mixture was stirred under hydrogen atmosphere for 15 h. The catalyst was filtered off, the solvent was removed under reduced to obtain product **10** (0.872 g) as a brown solid. Yield 98% (0.872 g); mp 152–156 °C; ^{1}H NMR (400 MHz, DMSO-d_6) δ 1.87 (s, 3H, CH$_3$), 6.16 (br s, 2H, NH$_2$), 6.60 (d, 1H, J = 8.4 Hz, Ar-H-3,5), 7.53 (d, 1H, J = 8.4 Hz, Ar-H-2,6), 11.64 (s, 1H, NH).

4.1.13. General procedure E. Synthesis of compounds 12a-e, 14a-c, 14e-i, 15a, 15b, 19, 29a-d, 30, 31a-c, 32a-c (with 12a as an example)

To the solution of **3a** (50.0 mg, 0.267 mmol) in anhydrous dichloromethane (3 mL) oxalyl chloride (2 M solution in dichloromethane, 268 μL, 0.534 mmol) was added and the mixture was stirred under an argon atmosphere for 15 h. The solvent was removed under reduced pressure, to the residue anhydrous dichloromethane (2 mL), pyridine (1 mL) and compound **10** (57.2 mg, 0.267 mmol) were added and stirred at rt for 15 h. The solvent was removed in vacuo and the residue dissolved in ethyl acetate (30 mL) and 1 M HCl (10 mL). Organic phase was washed with 1 M HCl (2 × 10 mL) and brine (2 × 10 mL), dried over Na$_2$SO$_4$ and evaporated under reduced pressure. To the crude product ether (10 mL) was added, the obtained suspension was sonicated, filtered, washed with ether (2 × 5 mL) and dried to afford **12a** (74 mg) as a white solid.

4.1.14. N-(4-(N-Acetylsulfamoyl)phenyl)-1-phenyl-1H-pyrrole-2-carboxamide (12a)

Synthesized according to General procedure E. White solid; yield 72% (74 mg); mp 241–243 °C; IR (ATR) ν = 3344, 3116, 2890, 1700, 1647, 1592, 1526, 1513, 1496, 1446, 1409, 1351, 1320, 1304, 1271, 1230, 1159, 1112, 1097, 1050, 1000, 850, 831 cm^{-1}. ^{1}H NMR (400 MHz, DMSO-d_6) δ 1.91 (s, 3H, CH$_3$), 6.36 (dd, 1H, J = 3.9, 2.7 Hz, pyrr-H), 7.16 (dd, 1H, J = 3.9, 1.7 Hz, pyrr-H), 7.25 (dd, 1H, J = 2.7, 1.6 Hz, pyrr-H), 7.29–7.41 (m, 3H, Ar–H), 7.44 (t, 2H, J = 7.5 Hz, Ar–H), 7.77–7.91 (m, 4H, Ar–H), 10.48 (s, 1H, NH), 11.97 (s, 1H, NH); ^{13}C NMR (100 MHz, DMSO-d_6) δ 23.16 (CH$_3$), 108.75, 116.16, 118.98, 125.19, 126.21, 127.02, 128.66, 128.72, 129.16, 132.59, 140.13, 144.01, 159.23, 168.62 (C=O); MS (ESI) m/z (%) = 384.1 (MH$^+$), HRMS for C$_{19}$H$_{18}$N$_3$O$_4$S: calculated 384.1018, found 384.1016; HPLC: Phenomenex Luna 5 μm C18 column (4.6 mm × 150 mm); mobile phase: 30–90% acetonitrile in TFA (0.1%) in 16 min, 90% acetonitrile to 20 min; flow rate 1.0 mL/min; injection volume: 10 μL; retention time: 8.786 min (98.2% at 280 nm).

4.1.15. N-(4-(N-Acetylsulfamoyl)phenyl)-1-benzyl-1H-pyrrole-2-carboxamide (12b)

Synthesized according to General procedure E from **3c** (25 mg, 0.124 mmol) and **10** (27 mg, 0.124 mmol). White solid; yield 93% (44 mg); mp 189–190 °C; IR (ATR) ν = 3372, 3137, 2909, 1701, 1648, 1589, 1533, 1518, 1460, 1412, 1401, 1353, 1339, 1308, 1245, 1227, 1180, 1167, 1157, 1094, 994, 846, 830 cm^{-1}. ^{1}H NMR (400 MHz, DMSO-d_6) δ 1.91 (s, 3H, CH$_3$), 5.62 (s, 2H, CH$_2$), 6.22 (dd, 1H, J = 4.0, 2.6 Hz, pyrr-H), 7.06–7.18 (m, 3H, Ar–H), 7.19–7.36 (m, 4H, Ar–H), 7.83 (d, 2H, J = 9.0 Hz, Ar-H-3,5), 7.90 (d, 2H, J = 9.0 Hz, Ar-H-2,6), 10.20 (s, 1H, NH), 11.97 (s, 1H, NH); ^{13}C NMR (100 MHz, DMSO-d_6) δ 23.17 (CH$_3$), 50.93 (CH$_2$), 107.69, 115.52, 119.15, 124.26, 126.67, 127.11, 128.39, 128.65, 129.45, 132.54, 139.19, 143.97, 159.88, 168.63 (C=O); MS (ESI) m/z (%) = 398.1 (MH$^+$), HRMS for C$_{20}$H$_{20}$N$_3$O$_4$S: calculated 398.1175, found 398.1172; HPLC: Phenomenex Luna 5 μm C18 column (4.6 mm × 150 mm); mobile phase: 30–90% acetonitrile in TFA (0.1%) in 16 min, 90% acetonitrile to 20 min; flow rate 1.0 mL/min; injection volume: 10 μL; retention time: 10.061 min (99.7% at 280 nm).

4.1.16. *N-(4-(N-Acetylsulfamoyl)phenyl)-1-(4-chlorobenzyl)-1H-pyrrole-2-carboxamide (12c)*

Synthesized according to General procedure E from **3b** (60 mg, 0.255 mmol) and **10** (55 mg, 0.255 mmol). White solid; yield 74% (81 mg); mp 229–231 °C; IR (ATR) ν = 3368, 3261, 3122, 3052, 2890, 1714, 1666, 1588, 1536, 1520, 1496, 1445, 1416, 1400, 1364, 1342, 1331, 1249, 1226, 1150, 1101, 1087, 1014, 1000, 853 cm^{-1}. ^{1}H NMR (400 MHz, DMSO-d_6) δ 1.91 (s, 3H, CH$_3$), 5.60 (s, 2H, CH$_2$), 6.24 (dd, 1H, J = 4.0, 2.6 Hz, pyrr-H), 7.13 (d, 2H, J = 8.3 Hz, Ar–H), 7.18 (dd, 1H, J = 4.0, 1.7 Hz, pyrr-H), 7.25–7.33 (m, 1H, pyrr-H), 7.37 (d, 2H, J = 8.3 Hz, Ar–H), 7.84 (d, 2H, J = 8.8 Hz, Ar–H), 7.89 (d, 2H, J = 8.8 Hz, Ar–H), 10.19 (s, 1H, NH), 11.98 (s, 1H, NH); ^{13}C NMR (100 MHz, DMSO-d_6) δ 23.17 (CH$_3$), 50.37 (CH$_2$), 107.95, 115.63, 119.27, 124.04, 128.35, 128.50, 128.59, 129.53, 131.70, 132.66, 138.16, 143.79, 159.80, 168.92 (C=O); MS (ESI) m/z (%) = 430.1 ([M − H]$^-$), HRMS for C$_{20}$H$_{17}$N$_3$O$_4$SCl: calculated 430.0628, found 430.0619; HPLC: Phenomenex Luna 5 μm C18 column (4.6 mm × 150 mm); mobile phase: 30–90% acetonitrile in TFA (0.1%) in 16 min, 90% acetonitrile to 20 min; flow rate 1.0 mL/min; injection volume: 10 μL; retention time: 11.271 min (97.6% at 280 nm).

4.1.17. *N-(4-(N-Acetylsulfamoyl)phenyl)-4,5-dibromo-1-phenyl-1H-pyrrole-2-carboxamide (12d)*

Synthesized according to General procedure E from **3d** (30 mg, 0.087 mmol) and **10** (19 mg, 0.087 mmol). White solid; yield 59% (28 mg); mp 212–214 °C; IR (ATR) ν = 3371, 3217, 1698, 1660, 1591, 1529, 1511, 1497, 1444, 1421, 1405, 1358, 1346, 1311, 1246, 1228, 1161, 1095, 1030, 998, 965, 849, 829 cm^{-1}. ^{1}H NMR (400 MHz, DMSO-d_6) δ 1.89 (s, 3H, CH$_3$), 7.26–7.37 (m, 2H, Ar–H), 7.46 (s, 1H, pyrr-H), 7.48–7.57 (m, 3H, Ar–H), 7.78–7.83 (m, 4H, Ar–H), 10.42 (s, 1H, NH), 11.97 (s, 1H, NH); ^{13}C NMR (100 MHz, DMSO-d_6) δ 23.15 (CH$_3$), 98.91, 112.94, 116.43, 119.12, 127.93, 128.69, 128.79, 128.83, 128.92, 133.01, 138.59, 143.42, 157.18, 168.62 (C=O); MS (ESI) m/z (%) = 539.9 ([M − H]$^-$), HRMS for C$_{19}$H$_{14}$N$_3$O$_4$SBr$_2$: calculated 537.9072, found 537.9065; HPLC: Phenomenex Luna 5 μm C18 column (4.6 mm × 150 mm); mobile phase: 30–90% acetonitrile in TFA (0.1%) in 16 min, 90% acetonitrile to 20 min; flow rate 1.0 mL/min; injection volume: 10 μL; retention time: 12.183 min (98.9% at 280 nm).

4.1.18. *N-(4-(N-Acetylsulfamoyl)phenyl)-1-benzyl-4,5-dibromo-1H-pyrrole-2-carboxamide (12e)*

Synthesized according to General procedure E from **3e** (60 mg, 0.167 mmol) and **10** (36 mg, 0.167 mmol). White solid; yield 67% (62 mg); mp 215–216 °C; IR (ATR) ν = 3546, 3307, 3215, 3121, 2861, 1731, 1699, 1656, 1590, 1533, 1495, 1448, 1413, 1402, 1391, 1337, 1309, 1242, 1158, 1096, 1045, 1010, 949, 886, 853, 832 cm^{-1}. ^{1}H NMR (400 MHz, DMSO-d_6) δ 1.91 (s, 3H, CH$_3$), 5.76 (s, 2H, CH$_2$), 7.03 (d, 2H, J = 6.7 Hz, Ar–H), 7.24–7.27 (m, 1H, Ar–H), 7.33 (t, 2H, J = 7.3 Hz, Ar–H), 7.45 (s, 1H, pyrr-H), 7.81–7.94 (m, 4H, Ar–H), 10.41 (s, 1H, NH), 12.00 (s, 1H, NH); ^{13}C NMR (100 MHz, DMSO-d_6) δ 23.16 (CH$_3$), 50.44 (CH$_2$), 98.32, 112.83, 116.87, 119.42, 126.11, 127.01, 127.25, 128.59, 128.72, 133.18, 137.25, 143.36, 158.28, 168.64 (C=O); MS (ESI) m/z (%) = 551.9 ([M − H]$^-$), HRMS for C$_{20}$H$_{16}$N$_3$O$_4$SBr$_2$: calculated 551.9228, found 551.9221; HPLC: Phenomenex Luna 5 μm C18 column (4.6 mm × 150 mm); mobile phase: 30–90% acetonitrile in TFA (0.1%) in 16 min, 90% acetonitrile to 20 min; flow rate 1.0 mL/min; injection volume: 10 μL; retention time: 13.223 min (99.7% at 280 nm).

4.1.19. *(1R,2R)-N-(4-(N-Acetylsulfamoyl)phenyl)-2-phenylcyclopropane-1-carboxamide (13)*

To a solution of (1*R*,2*R*)-2-phenylcyclopropane-1-carboxylic acid (**11a**, 100 mg, 0.617 mmol) and TBTU (216 mg, 0.673 mmol) in DMF (5 mL) *N*-methylmorpholine (185 μL, 1.68 mmol) was added and the solution was stirred at rt for 0.5 h. Compound **10** (120 mg, 0.561 mmol) was added and the mixture was stirred at 50 °C for 15 h. The solvent was removed in vacuo and the residue dissolved in ethyl acetate (30 mL) and

1 M HCl (10 mL). Organic phase was washed with 1 M HCl (3 × 10 mL) and brine (2 × 10 mL), dried over Na$_2$SO$_4$ and evaporated under reduced pressure. The crude product was purified with flash column chromatography using ethyl acetate/petroleum ether (1:1 to 2:1) as solvent. To the residue ether (5 mL) was added, the obtained suspension was sonicated, filtered, washed with ether (5 mL) and dried to afford **13** (50 mg) as a white solid. Yield 25% (50 mg); mp 209–211 °C; IR (ATR) ν = 3294, 3098, 2878, 1711, 1656, 1588, 1533, 1463, 1431, 1411, 1340, 1311, 1232, 1161, 1095, 1081, 1027, 1000, 952, 934, 856, 833 cm-1 [α]$_D^{25}$ +4.35 (*c* 0.207, DMF); ^{1}H NMR (400 MHz, DMSO-d_6) δ 1.41–1.46 (m, 1H, CH), 1.51–1.56 (m, 1H, CH), 1.91 (s, 3H, CH$_3$), 2.10–2.14 (m, 1H, CH), 2.39–2.44 (m, 1H, CH), 7.19–7.23 (m, 3H, Ar–H), 7.29–7.33 (m, 2H, Ar–H), 7.80 (d, 2H, J = 9.0 Hz, Ar–H), 7.85 (d, 2H, J = 9.0 Hz, Ar–H), 10.72 (s, 1H, NH), 11.99 (s, 1H, NH); ^{13}C NMR (100 MHz, DMSO-d_6) δ 15.97 (CH$_2$), 23.17 (CH$_3$), 25.48 (CH), 26.84 (CH), 118.34, 125.90, 126.21, 128.37, 128.93, 132.73, 140.50, 143.58, 168.65 (C=O), 170.64 (C=O); MS (ESI) m/z (%) = 359.1 (MH$^+$), HRMS for C$_{18}$H$_{19}$N$_2$O$_4$S: calculated 359.1066, found 359.1061; HPLC: Phenomenex Luna 5 μm C18 column (4.6 mm × 150 mm); mobile phase: 30–90% acetonitrile in TFA (0.1%) in 16 min, 90% acetonitrile to 20 min; flow rate 1.0 mL/min; injection volume: 10 μL; retention time: 8.723 min (100% at 280 nm).

4.1.20. *1-Phenyl-N-(3-(N-(thiazol-2-yl)sulfamoyl)phenyl)-1H-pyrrole-2-carboxamide (14a)*

Synthesized according to General procedure E from **3a** (26 mg, 0.141 mmol) and **6a** (36 mg, 0.141 mmol). Pale yellow solid; yield 50% (30 mg); mp 208–210 °C; IR (ATR) ν = 3328, 3110, 2895, 1679, 1596, 1563, 1530, 1498, 1477, 1447, 1417, 1360, 1308, 1288, 1264, 1241, 1145, 1125, 1096, 1073, 1042, 941, 862 cm^{-1}. ^{1}H NMR (400 MHz, DMSO-d_6) δ 6.34 (dd, 1H, J = 3.9, 2.5 Hz, pyrr-H), 6.83 (d, 1H, J = 4.6 Hz, thiazole-H), 7.13–7.46 (m, 10H, Ar–H), 7.81 (dt, 1H, J = 7.1, 2.1 Hz, Ar–H), 8.22 (t, 1H, J = 1.8 Hz, Ar–H), 10.33 (s, 1H, NH), 12.77 (s, 1H, NH); ^{13}C NMR (100 MHz, DMSO-d_6) δ 108.25, 108.67, 115.72, 116.71, 120.14, 122.68, 124.38, 125.21, 126.39, 126.97, 128.70, 128.82, 129.03, 139.81, 140.24, 142.59, 159.14, 168.84 (C=O); MS (ESI) m/z (%) = 423.0 ([M − H]$^-$), HRMS for C$_{20}$H$_{15}$N$_4$O$_3$S$_2$: calculated 423.0586, found 423.0584; HPLC: Phenomenex Luna 5 μm C18 column (4.6 mm × 150 mm); mobile phase: 30–90% acetonitrile in TFA (0.1%) in 16 min, 90% acetonitrile to 20 min; flow rate 1.0 mL/min; injection volume: 10 μL; retention time: 8.630 min (96.8% at 280 nm).

4.1.21. *1-Phenyl-N-(4-(N-(thiazol-2-yl)sulfamoyl)phenyl)-1H-pyrrole-2-carboxamide (14b)*

Synthesized according to General procedure E from **3a** (50 mg, 0.267 mmol) and **6b** (68 mg, 0.267 mmol). White solid; yield 64% (72 mg); mp 249–251 °C; IR (ATR) ν = 3376, 3116, 3016, 2864, 2774, 1671, 1581, 1541, 1511, 1497, 1452, 1413, 1400, 1366, 1313, 1294, 1263, 1247, 1220, 1146, 1125, 1089, 1047, 932, 861, 828 cm^{-1}. ^{1}H NMR (400 MHz, DMSO-d_6) δ 6.34 (dd, 1H, J = 3.8, 2.6 Hz, pyrr-H), 6.81 (d, 1H, J = 4.6 Hz, thiazole-H), 7.13 (dd, 1H, J = 3.9, 1.7 Hz, Ar–H), 7.22–7.46 (m, 7H, Ar–H), 7.71 (d, 2H, J = 8.8 Hz, Ar–H), 7.78 (d, 2H, J = 8.8 Hz, Ar–H), 10.37 (s, 1H, NH), 12.69 (s, 1H, NH); ^{13}C NMR (100 MHz, DMSO-d_6) δ 108.05, 108.68, 115.90, 119.05, 124.40, 125.19, 126.35, 126.74, 126.98, 128.69, 128.96, 135.96, 140.18, 142.61, 159.12, 168.65 (C=O); MS (ESI) m/z (%) = 425.1 (MH$^+$), HRMS for C$_{20}$H$_{17}$N$_4$O$_3$S$_2$: calculated 425.0742, found 425.0747; HPLC: Phenomenex Luna 5 μm C18 column (4.6 mm × 150 mm); mobile phase: 30–90% acetonitrile in TFA (0.1%) in 16 min, 90% acetonitrile to 20 min; flow rate 1.0 mL/min; injection volume: 10 μL; retention time: 8.488 min (96.5% at 280 nm).

4.1.22. *1-Benzyl-N-(3-(N-(thiazol-2-yl)sulfamoyl)phenyl)-1H-pyrrole-2-carboxamide (14c)*

Synthesized according to General procedure E from **3b** (25 mg, 0.124 mmol) and **6a** (32 mg, 0.124 mmol). Pale yellow solid; yield 46%

(25 mg); mp 172–175 °C; IR (ATR) ν = 3361, 3104, 3027, 2810, 1663, 1573, 1530, 1519, 1474, 1460, 1416, 1317, 1288, 1232, 1140, 1121, 1102, 1085, 942 cm^{-1}. ^{1}H NMR (400 MHz, DMSO-d_6) δ 5.63 (s, 2H, CH$_2$), 6.19–6.22 (m, 1H, pyrr-H), 6.84 (d, 1H, J = 4.6 Hz, thiazole-H), 7.10–7.15 (m, 3H, Ar–H), 7.20–7.31 (m, 5H, Ar–H), 7.42–7.46 (m, 2H, Ar–H), 7.84–7.88 (m, 1H, Ar–H), 8.27 (s, 1H, Ar–H), 10.05 (s, 1H, NH), 12.77 (s, 1H, NH); ^{13}C NMR (100 MHz, DMSO-d_6) δ 50.88 (CH$_2$), 107.61, 108.26, 114.97, 116.92, 120.09, 122.90, 124.38, 126.64, 127.07, 128.38, 129.05, 139.31, 139.74, 142.58, 159.82, 168.86 (C=O), signals for two carbon atoms not seen; MS (ESI) m/z (%) = 439.1 (MH$^+$), HRMS for C$_{21}$H$_{19}$N$_4$O$_3$S$_2$: calculated 439.0899, found 439.0893; HPLC: Phenomenex Luna 5 μm C18 column (4.6 mm × 150 mm); mobile phase: 30–90% acetonitrile in TFA (0.1%) in 16 min, 90% acetonitrile to 20 min; flow rate 1.0 mL/min; injection volume: 10 μL; retention time: 9.849 min (97.6% at 280 nm).

4.1.23. 1-Benzyl-N-(4-(N-(thiazol-2-yl)sulfamoyl)phenyl)-1H-pyrrole-2-carboxamide (14d)

To a solution of **3b** (87 mg, 0.431 mmol) and TBTU (163 mg, 0.509 mmol) in DMF (5 mL) *N*-methylmorpholine (129 μL, 1.18 mmol) was added and the solution was stirred at rt for 0.5 h. 4-Amino-*N*-(thiazol-2-yl)benzenesulfonamide (**6b**, 100 mg, 0.392 mmol) was added and the mixture was stirred at 50 °C for 15 h. The solvent was removed in vacuo and the residue dissolved in ethyl acetate (50 mL) and 1 M HCl (20 mL). Organic phase was washed with 1 M HCl (3 × 20 mL) and brine (2 × 15 mL), dried over Na$_2$SO$_4$ and evaporated under reduced pressure. To the residue ether (5 mL) was added, the obtained suspension was sonicated, filtered, washed with ether (5 mL) and dried. The crude product was purified with flash column chromatography using dichloromethane/methanol (50:1 to 20:1) as solvent to afford **14d** (50 mg) as an off-white solid. Yield 17% (30 mg); mp 190–193 °C; IR (ATR) ν = 3350, 3252, 3105, 1639, 1589, 1569, 1526, 1463, 1452, 1439, 1413, 1396, 1328, 1305, 1287, 1254, 1142, 1108, 1086, 926 cm^{-1}. ^{1}H NMR (400 MHz, DMSO-d_6) δ 5.61 (s, 2H, CH$_2$), 6.21 (dd, 1H, J = 3.9, 2.6 Hz, pyrr-H), 6.81 (d, 1H, J = 4.6 Hz, thiazole-H), 7.10–7.13 (m, 3H, Ar–H), 7.20–7.31 (m, 5H, Ar–H), 7.73 (d, 2H, J = 8.9 Hz, Ar–H), 7.83 (d, 2H, J = 8.9 Hz, Ar–H), 10.09 (s, 1H, NH), 12.68 (s, 1H, NH); ^{13}C NMR (100 MHz, DMSO-d_6) δ 50.88 (CH$_2$), 107.64, 108.04, 115.22, 119.26, 124.37, 126.65, 126.72, 126.80, 127.08, 128.37, 129.22, 135.95, 139.24, 142.55, 159.80, 168.67 (C=O); MS (ESI) m/z (%) = 439.1 (MH$^+$), HRMS for C$_{21}$H$_{19}$N$_4$O$_3$S$_2$: calculated 439.0899, found 439.0896; HPLC: Phenomenex Luna 5 μm C18 column (4.6 mm × 150 mm); mobile phase: 30–90% acetonitrile in TFA (0.1%) in 16 min, 90% acetonitrile to 20 min; flow rate 1.0 mL/min; injection volume: 10 μL; retention time: 9.728 min (96.0% at 280 nm).

4.1.24. 1-(4-Chlorobenzyl)-N-(3-(N-(thiazol-2-yl)sulfamoyl)phenyl)-1H-pyrrole-2-carboxamide (14e)

Synthesized according to General procedure E from **3c** (30 mg, 0.127 mmol) and **6a** (33 mg, 0.127 mmol). White solid; yield 42% (25 mg); mp 170–172 °C; IR (ATR) ν = 3364, 3114, 2810, 1666, 1580, 1535, 1484, 1462, 1417, 1397, 1327, 1304, 1282, 1241, 1137, 1117, 1121, 1016, 954, 859 cm^{-1}. ^{1}H NMR (400 MHz, DMSO-d_6) δ 5.61 (s, 2H, CH$_2$), 6.20–6.22 (m, 1H, pyrr-H), 6.84 (d, 1H, J = 4.5 Hz, thiazole-H), 7.12–7.17 (m, 3H, Ar–H), 7.25–7.27 (m, 2H, Ar–H), 7.37 (d, 2H, J = 8.1 Hz, Ar–H), 7.44–7.46 (m, 2H, Ar–H), 7.85–7.88 (m, 1H, Ar–H), 8.26 (s, 1H, Ar–H), 10.05 (s, 1H, NH), 12.77 (s, 1H, NH); ^{13}C NMR (100 MHz, DMSO-d_6) δ 50.30 (CH$_2$), 107.78, 108.25, 115.08, 116.94, 120.12, 122.93, 124.24, 124.41, 128.36, 128.52, 129.04, 129.09, 131.65, 138.36, 139.68, 142.59, 159.71, 168.87 (C=O); MS (ESI) m/z (%) = 471.0 ([M − H]$^-$), HRMS for C$_{21}$H$_{16}$N$_4$O$_3$S$_2$Cl: calculated 471.0352, found 471.0354; HPLC: Phenomenex Luna 5 μm C18 column (4.6 mm × 150 mm); mobile phase: 30–90% acetonitrile in TFA (0.1%) in 16 min, 90% acetonitrile to 20 min; flow rate 1.0 mL/min; injection volume: 10 μL; retention time: 11.029 min (96.2% at 280 nm).

4.1.25. 1-(4-Chlorobenzyl)-N-(4-(N-(thiazol-2-yl)sulfamoyl)phenyl)-1H-pyrrole-2-carboxamide (14f)

Synthesized according to General procedure E from **3c** (60 mg, 0.255 mmol) and **6b** (65 mg, 0.255 mmol). White solid; yield 76% (91 mg); mp 195–197 °C; IR (ATR) ν = 3363, 3116, 3018, 2806, 1666, 1577, 1538, 1530, 1510, 1490, 1460, 1410, 1325, 1310, 1291, 1245, 1145, 1119, 1088, 1014, 937, 850, 827, 801 cm^{-1}. ^{1}H NMR (400 MHz, DMSO-d_6) δ 5.59 (s, 2H, CH$_2$), 6.22 (dd, 1H, J = 4.0, 2.6 Hz, pyrr-H), 6.82 (d, 1H, J = 4.6 Hz, thiazole-H), 7.11–7.16 (m, 3H, Ar–H), 7.25–7.27 (m, 2H, Ar–H), 7.36 (d, 2H, J = 8.4 Hz, Ar–H), 7.73 (d, 2H, J = 8.9 Hz, Ar–H), 7.82 (d, 2H, J = 8.9 Hz, Ar–H), 10.09 (s, 1H, NH), 12.69 (s, 1H, NH); ^{13}C NMR (100 MHz, DMSO-d_6) δ 50.30 (CH$_2$), 107.80, 108.02, 115.33, 119.31, 124.24, 124.35, 126.72, 128.35, 128.54, 129.25, 131.66, 136.00, 138.28, 142.49, 159.69, 168.68; MS (ESI) m/z (%) = 471.0 ([M − H]$^-$), HRMS for C$_{21}$H$_{16}$N$_4$O$_3$S$_2$Cl: calculated 471.0355, found 471.0354; HPLC: Phenomenex Luna 5 μm C18 column (4.6 mm × 150 mm); mobile phase: 30–90% acetonitrile in TFA (0.1%) in 16 min, 90% acetonitrile to 20 min; flow rate 1.0 mL/min; injection volume: 10 μL; retention time: 10.928 min (98.5% at 280 nm).

4.1.26. 4,5-Dibromo-1-phenyl-N-(4-(N-(thiazol-2-yl)sulfamoyl)phenyl)-1H-pyrrole-2-carboxamide (14g)

Synthesized according to General procedure E from **3d** (30 mg, 0.087 mmol) and **6b** (22 mg, 0.087 mmol). White solid; yield 49% (25 mg); mp 227–230 °C; IR (ATR) ν = 3224, 1650, 1588, 1560, 1542, 1519, 1494, 1401, 1348, 1326, 1314, 1280, 1257, 1241, 1141, 1090, 1069, 968, 941, 866, 855 cm^{-1}. ^{1}H NMR (400 MHz, DMSO-d_6) δ 6.81 (d, 1H, J = 4.6 Hz, thiazole-H), 7.24 (d, 1H, J = 4.6 Hz, thiazole-H), 7.29–7.31 (m, 2H, Ar–H), 7.43 (s, 1H, pyrr-H), 7.47–7.51 (m, 3H, Ar–H), 7.68–7.73 (m, 4H, Ar–H), 10.31 (s, 1H, NH), 12.69 (s, 1H, NH); ^{13}C NMR (100 MHz, DMSO-d_6) δ 98.85, 108.06, 112.72, 116.21, 119.18, 124.40, 126.77, 127.94, 128.76, 128.80, 129.05, 136.39, 138.63, 142.02, 157.06, 168.69 (C=O); MS (ESI) m/z (%) = 578.9 ([M − H]$^-$), HRMS for C$_{20}$H$_{13}$N$_4$O$_3$S$_2$Br$_2$: calculated 578.8796, found 578.8788; HPLC: Phenomenex Luna 5 μm C18 column (4.6 mm × 150 mm); mobile phase: 30–90% acetonitrile in TFA (0.1%) in 16 min, 90% acetonitrile to 20 min; flow rate 1.0 mL/min; injection volume: 10 μL; retention time: 11.811 min (98.6% at 280 nm).

4.1.27. 1-Benzyl-4,5-dibromo-N-(3-(N-(thiazol-2-yl)sulfamoyl)phenyl)-1H-pyrrole-2-carboxamide (14h)

Synthesized according to General procedure E from **3e** (30 mg, 0.084 mmol) and **6a** (21 mg, 0.084 mmol). White solid; yield 62% (25 mg); mp 130–132 °C; IR (ATR) ν = 3275, 3107, 2814, 1651, 1582, 1533, 1498, 1418, 1324, 1301, 1282, 1258, 1144, 1126, 1084, 944, 857 cm^{-1}. ^{1}H NMR (400 MHz, DMSO-d_6) δ 5.76 (s, 2H, CH$_2$), 6.84 (d, 1H, J = 4.5 Hz, thiazole-H), 7.02–7.04 (m, 2H, Ar–H), 7.23–7.35 (m, 4H, Ar–H), 7.44–7.50 (m, 3H, Ar–H), 7.85 (dt, 1H, J = 7.0, 2.1 Hz, Ar–H), 8.25 (t, 1H, J = 1.5 Hz, Ar–H), 10.27 (s, 1H, NH), 12.77 (s, 1H, NH); ^{13}C NMR (100 MHz, DMSO-d_6) δ 50.39 (CH$_2$), 98.24, 108.30, 112.39, 116.45, 117.05, 120.65, 122.98, 124.44, 126.10, 127.13, 127.21, 128.58, 129.22, 137.34, 139.19, 142.68, 158.18, 168.88 (C=O); MS (ESI) m/z (%) = 592.9 ([M − H]$^-$), HRMS for C$_{21}$H$_{15}$N$_4$O$_3$S$_2$Br$_2$: calculated 592.8952, found 592.8959; HPLC: Phenomenex Luna 5 μm C18 column (4.6 mm × 150 mm); mobile phase: 30–90% acetonitrile in TFA (0.1%) in 16 min, 90% acetonitrile to 20 min; flow rate 1.0 mL/min; injection volume: 10 μL; retention time: 12.874 min (96.7% at 280 nm).

4.1.28. 1-Benzyl-4,5-dibromo-N-(4-(N-(thiazol-2-yl)sulfamoyl)phenyl)-1H-pyrrole-2-carboxamide (14i)

Synthesized according to General procedure E from **3e** (50 mg, 0.139 mmol) and **6b** (36 mg, 0.139 mmol). White solid; yield 47% (39 mg); mp 226–229 °C; IR (ATR) ν = 3110, 1681, 1645, 1588, 1561, 1518, 1496, 1437, 1403, 1327, 1311, 1300, 1277, 1256, 1243, 1203, 1141, 1089, 939, 855, 836 cm^{-1}. ^{1}H NMR (400 MHz, DMSO-d_6) δ 5.75 (s, 2H, CH$_2$), 6.82 (d, 1H, J = 4.8 Hz, thiazole-H), 7.01–7.04 (m, 2H, Ar–H),

7.23–7.26 (m, 2H, Ar–H), 7.31–7.35 (m, 2H, Ar–H), 7.43 (s, 1H, pyrr-H), 7.74 (d, 2H, J = 8.9 Hz, Ar–H), 7.81 (d, 2H, J = 8.9 Hz, Ar–H), 10.31 (s, 1H, NH), 12.71 (s, 1H, NH); ^{13}C NMR (100 MHz, DMSO-d_6) δ 50.40 (CH$_2$), 98.26, 108.08, 112.58, 116.63, 119.51, 124.36, 126.10, 126.80, 127.13, 127.22, 128.58, 136.58, 137.29, 141.95, 158.18, 168.72 (C=O); MS (ESI) m/z (%) = 593.0 ([M – H]$^-$), HRMS for C$_{21}$H$_{15}$N$_4$O$_3$S$_2$Br$_2$: calculated 592.8952, found 592.8956; HPLC: Phenomenex Luna 5 μm C18 column (4.6 mm × 150 mm); mobile phase: 30–90% acetonitrile in TFA (0.1%) in 16 min, 90% acetonitrile to 20 min; flow rate 1.0 mL/min; injection volume: 10 μL; retention time: 12.874 min (97.4% at 280 nm).

4.1.29. (1R,2R)-2-phenyl-N-(3-(N-(thiazol-2-yl)sulfamoyl)phenyl) cyclopropane-1-carboxamide (15a)

Synthesized according to General procedure E from **11a** (20 mg, 0.123 mmol) and **6a** (32 mg, 0.123 mmol). Off-white solid; yield 28% (14 mg); mp 111–113 °C; IR (ATR) ν = 3312, 3109, 1665, 1595, 1568, 1526, 1478, 1417, 1327, 1290, 1191, 1135, 1095, 1081, 937, 853 cm-1 [α]$_D^{25}$ − 4.19 (c 0.215, DMF); ^{1}H NMR (400 MHz, DMSO-d_6) δ 1.40 (ddd, 1H, J = 7.9, 6.3, 4.2 Hz, CH), 1.52 (dt, 1H, J = 9.2, 4.9 Hz, CH), 2.06 (ddd, 1H, J = 9.0, 5.3, 4.0 Hz, CH), 2.39 (ddd, 1H, J = 9.7, 6.3, 4.0 Hz, CH), 6.84 (d, 1H, J = 4.6 Hz, thiazole-H), 7.19–7.23 (m, 3H, Ar–H), 7.26–7.33 (m, 3H, Ar–H), 7.45–7.46 (m, 2H, Ar–H), 7.71 (td, 1H, J = 4.6, 2.1 Hz, Ar–H), 8.21 (d, 1H, J = 1.3 Hz, Ar–H), 10.55 (s, 1H, NH), 12.78 (s, 1H, NH); ^{13}C NMR (100 MHz, DMSO-d_6) δ 15.74 (CH$_2$), 25.15 (CH), 26.74 (CH), 108.29, 115.95, 120.17, 121.77, 124.51, 125.90, 126.16, 128.36, 129.36, 139.52, 140.61, 142.82, 168.90, 170.25 (C=O); MS (ESI) m/z (%) = 400.1 (MH$^+$), HRMS for C$_{19}$H$_{18}$N$_3$O$_3$S$_2$: calculated 400.0790, found 400.0785; HPLC: Phenomenex Luna 5 μm C18 column (4.6 mm × 150 mm); mobile phase: 30–90% acetonitrile in TFA (0.1%) in 16 min, 90% acetonitrile to 20 min; flow rate 1.0 mL/min; injection volume: 10 μL; retention time: 8.518 min (96.6% at 280 nm).

4.1.30. 2-(3,4-Difluorophenyl)-N-(4-(N-(thiazol-2-yl)sulfamoyl)phenyl) cyclopropane-1-carboxamide (15b)

Synthesized according to General procedure E from **11b** (100 mg, 0.505 mmol) and **6b** (129 mg, 0.505 mmol). White solid; yield 68% (150 mg); mp 116–118 °C; IR (ATR) ν = 3311, 3112, 3029, 2814, 1683, 1589, 1519, 1421, 1404, 1328, 1296, 1276, 1177, 1140, 1089, 938, 855, 839, 812 cm^{-1}. ^{1}H NMR (400 MHz, DMSO-d_6) δ 1.45 (ddd, 1H, J = 8.2, 6.3, 4.3 Hz, CH), 1.51 (dt, 1H, J = 9.3, 5.0 Hz, CH), 2.06–2.10 (m, 1H, CH), 2.43 (ddd, 1H, J = 9.7, 6.2, 3.9 Hz, CH), 6.82 (d, 1H, J = 4.6 Hz, thiazole-H), 7.07–7.10 (m, 1H, Ar–H), 7.25 (d, 1H, J = 4.6 Hz, thiazole-H), 7.25–7.37 (m, 2H, Ar–H), 7.73 (s, 4H, Ar–H), 10.60 (s, 1H, NH), 12.69 (s, 1H, NH); ^{13}C NMR (100 MHz, DMSO-d_6) δ 15.88, 24.41, 26.99, 108.06, 114.91 (d, J_{C-F} = 17.4 Hz, Ar-C-2′), 117.26 (d, J_{C-F} = 16.8 Hz, Ar-C-5′), 118.40 (s, Ar-C-2,6), 122.81 (dd, J_{C-F} = 6.2, 3.2 Hz, Ar-C-6′), 124.34, 126.97 (s, Ar-C-3,5), 136.18, 138.63 (dd, J_{C-F} = 6.3, 3.5 Hz, Ar-C-1′), 142.20, 147.95 (dd, J_{C-F} = 242, 12.6 Hz, Ar-C-4′), 149.38 (dd, J_{C-F} = 244, 12.7 Hz, Ar-C-3′), 168.67, 170.04 (s, C=O); MS (ESI) m/z (%) = 434.0 ([M – H]$^-$), HRMS for C$_{19}$H$_{14}$N$_3$O$_3$S$_2$F$_2$: calculated 434.0445, found 434.0453; HPLC: Phenomenex Luna 5 μm C18 column (4.6 mm × 150 mm); mobile phase: 30–90% acetonitrile in TFA (0.1%) in 16 min, 90% acetonitrile to 20 min; flow rate 1.0 mL/min; injection volume: 10 μL; retention time: 9.414 min (97.5% at 280 nm).

4.1.31. 4-Nitro-N-(thiazol-2-yl)benzamide (17) [62]

To a stirred solution of 4-nitrobenzoyl chloride (1.00 g, 5.39 mmol) in 1,2-dichloroethane (20 mL), a solution of 2-aminothiazole (360 mg, 3.59 mmol) and pyridine (289 μL, 3.59 mmol) in 1,2-dichloroethane (10 mL) was added dropwise, and the mixture was stirred at 60 °C for 15 h. The mixture was cooled on an ice bath, the precipitate was filtered off, washed with 1,2-dichloroethane (10 mL) and dried to obtain **17** (0.787 g) as a pale-yellow solid. Yield 88% (0.787 g); mp 190–195 °C; ^{1}H NMR (400 MHz, DMSO-d_6) δ 7.34 (d, 1H, J = 3.6 Hz, thiazole-H), 7.61 (d, 1H, J = 3.6 Hz, thiazole-H), 8.31 (d, 2H, J = 8.8 Hz, Ar–H), 8.38 (d, 2H, J =

8.9 Hz, Ar–H), 13.08 (s, 1H, NH).

4.1.32. 4-Amino-N-(thiazol-2-yl)benzamide (18) [63]

To a solution of compound **17** (0.700 g, 2.81 mmol) in a mixture of ethanol (40 mL), glacial acetic acid (5 mL) and tetrahydrofuran (5 mL) under argon Pd–C (100 mg) was added and the reaction mixture was stirred under hydrogen atmosphere for 15 h. The catalyst was filtered off and the solvent was removed under reduced pressure. To the residue ethyl acetate (50 mL) and saturated solution of NaHCO$_3$ (20 mL) were added, and the undissolved orange solid was removed by filtration and dried. The liquid phases were separated and organic phase was washed with brine (2 × 15 mL), dried over Na$_2$SO$_4$, filtered and the solvent evaporated under reduced pressure. The solids were combined to obtain product **18** (456 mg) as a pale-yellow solid. Yield 74% (456 mg); mp 222–224 °C; ^{1}H NMR (400 MHz, DMSO-d_6) δ 5.94 (s, 2H, NH$_2$), 6.60 (d, 2H, J = 8.7 Hz, Ar–H), 7.19 (d, 1H, J = 3.6 Hz, thiazole-H), 7.50 (d, 1H, J = 3.6 Hz, thiazole-H), 7.85 (d, 2H, J = 8.7 Hz, Ar–H), 12.05 (s, 1H, NH).

4.1.33. 4-((1R,2R)-2-phenylcyclopropane-1-carboxamido)-N-(thiazol-2-yl)benzamide (19)

Synthesized according to General procedure E from **11a** (73 mg, 0.450 mmol) and **18** (100 mg, 0.450 mmol). Pale yellow solid; yield 42% (69 mg); mp 228–231 °C; IR (ATR) ν = 3231, 3179, 3031, 1671, 1640, 1594, 1522, 1483, 1437, 1412, 1352, 1302, 1264, 1182, 1158, 1114, 1027, 960, 934, 895, 847 cm-1 [α]$_D^{25}$ +4.63 (c 0.289, DMF); ^{1}H NMR (400 MHz, DMSO-d_6) δ 1.43 (ddd, 1H, J = 8.2, 6.4, 4.2 Hz, CH), 1.54 (ddd, 1H, J = 9.2, 5.3, 4.2 Hz, CH), 2.10–2.15 (m, 1H, CH), 2.42 (ddd, 1H, J = 9.1, 6.3, 3.9 Hz, CH), 7.20–7.33 (m, 6H, Ar–H), 7.56 (d, 1H, J = 3.6 Hz, thiazole-H), 7.75 (d, 2H, J = 8.9 Hz, Ar–H), 8.08 (d, 2H, J = 8.9 Hz, Ar–H), 10.62 (s, 1H, NH), 12.50 (s, 1H, NH); ^{13}C NMR (100 MHz, DMSO-d_6) δ 15.86 (CH$_2$), 25.34 (CH), 26.88 (CH), 113.68, 118.11, 125.90, 126.18, 128.36, 129.25, 137.58, 140.57, 142.92, 158.79, 164.32, 170.44 (C=O), signals for two carbon atoms are overlapping; MS (ESI) m/z (%) = 364.1 (MH$^+$), HRMS for C$_{20}$H$_{18}$N$_3$O$_2$S: calculated 364.1120, found 364.1125; HPLC: Phenomenex Luna 5 μm C18 column (4.6 mm × 150 mm); mobile phase: 30–90% acetonitrile in TFA (0.1%) in 16 min, 90% acetonitrile to 20 min; flow rate 1.0 mL/min; injection volume: 10 μL; retention time: 10.478 min (97.2% at 280 nm).

4.1.34. Methanesulfonamide (21a) [64]

A solution of methanesulfonyl chloride (**20a**, 2 mL, 18.8 mmol) in tetrahydrofuran (30 mL) was saturated with NH$_{3(g)}$ and stirred at rt for 30 min. The mixture was cooled on an ice bath, precipitate was filtered off, washed with tetrahydrofuran (10 mL) and dried to obtain **21a** (1.43 g) as a white solid. Yield 80% (1.43 g); mp 75–79 °C; ^{1}H NMR (400 MHz, DMSO-d_6) δ 2.92 (s, 3H, CH$_3$), 6.82 (s, 2H, NH$_2$).

4.1.35. N,N-dimethylsulfamide (21b) [65]

N,N-Dimethylsulfamoyl chloride (**20b**, 1 mL, 9.40 mmol) was treated with 7 N ammonia in methanol (14 mL, 98 mmol) in a sealed high-pressure flask and heated at 60 °C for 15 h. Solvent was evaporated under reduced pressure, to the residue dichloromethane (15 mL) was added, the solid was filtered off, washed with dichloromethane (10 mL) and dried. To the solid residue tetrahydrofuran (15 mL) was added, the suspension was sonicated, the solid was filtered off, and washed with tetrahydrofuran (10 mL). The filtrate was evaporated under reduced pressure to obtain **21b** (0.553 g) as a white solid. Yield 47% (0.553 g); mp 83–86 °C; ^{1}H NMR (400 MHz, DMSO-d_6) δ 2.59 (s, 6H, CH$_3$), 6.70 (s, 2H, NH$_2$).

4.1.36. N-(Methylsulfonyl)-4-nitrobenzamide (22a) [66]

To a solution of compound **21a** (1.00 g, 10.5 mmol) in dry tetrahydrofuran (15 mL) cooled on an ice bath sodium hydride (403 mg, 10.5 mmol, 60% dispersion in mineral oil) was added portionwise. After 30 min a solution of 4-nitrobenzoyl chloride (0.975 g, 5.26 mmol) in

tetrahydrofurane 10 mL was added dropwise and the mixture was stirred for 1 h at rt and for 15 h at 50 °C. The solvent was removed under reduced pressure and to the residue ethyl acetate (50 mL) and 0.5 M HCl (20 mL) were added. The layers were separated, the organic phase was washed with 0.5 M HCl (2 × 20 mL) and brine (20 mL), dried over Na$_2$SO$_4$, filtered and evaporated under reduced pressure. To the solid residue ether (20 mL) was added, the suspension was sonicated, the solid was filtered off, washed with ether and dried to obtain **22a** (1.10 g) as a white solid. Yield 86% (1.10 g); mp 173–178 °C ^{1}H NMR (400 MHz, DMSO-d_6) δ 3.40 (s, 1H, CH$_3$, overlapping with the signal for water), 8.17 (d, 2H, J = 9.0 Hz, Ar–H), 8.35 (d, 2H, J = 9.0 Hz, Ar–H), 12.59 (br s, 1H, NH).

4.1.37. N-(N,N-Dimethylsulfamoyl)-4-nitrobenzamide (22b)

To a solution of compound **21b** (1.20 g, 9.67 mmol) in dry tetrahydrofuran (10 mL) cooled on an ice bath sodium hydride (387 mg, 9.67 mmol, 60% dispersion in mineral oil) was added portionwise. After 30 min a solution of 4-nitrobenzoyl chloride (1.20 g, 6.44 mmol) in tetrahydrofurane 10 mL was added dropwise and the mixture was stirred for 1 h at rt and for 15 h at 50 °C. The solvent was removed under reduced pressure and to the residue ethyl acetate (40 mL) and 0.5 M HCl (20 mL) were added. The layers were separated, the organic phase was washed with 0.5 M HCl (2 × 20 mL) and brine (20 mL), dried over Na$_2$SO$_4$, filtered and evaporated under reduced pressure. To the solid residue ether (20 mL) was added, the suspension was sonicated, the solid was filtered off, washed with ether and dried. The crude product was purified with flash column chromatography using dichloromethane/methanol (20:1) as solvent, to obtain **22b** (0.700 g) as white crystals. Yield 40% (700 mg); mp 159–164 °C; IR (ATR) ν = 3324, 3268, 3116, 2950, 1695, 1604, 1548, 1519, 1432, 1403, 1341, 1323, 1297, 1249, 1149, 1104, 1086, 978, 896, 867, 851, 819 cm^{-1}. ^{1}H NMR (400 MHz, DMSO-d_6) δ 2.85 (s, 6H, CH$_3$), 8.14 (d, 4H, J = 9.0 Hz, Ar–H), 8.31 (d, 5H, J = 9.0 Hz, Ar–H), 12.24 (s, 1H, NH); ^{13}C NMR (100 MHz, DMSO-d_6) δ 38.10 (CH$_3$), 123.39, 129.78, 139.24, 149.45, 165.02 (C=O); MS (ESI) m/z (%) = 272.0 ([M − H]$^-$), HRMS for C$_9$H$_{10}$N$_3$O$_5$S: calculated 272.0341, found 272.0343.

4.1.38. 4-Amino-N-(methylsulfonyl)benzamide (23a)

To a solution of compound **22a** (200 mg, 0.934 mmol) in a mixture of ethanol (5 mL) and glacial acetic acid (5 mL) under argon Pd–C (50 mg) was added and the reaction mixture was stirred under hydrogen atmosphere for 15 h. The catalyst was filtered off and the solvent was removed under reduced pressure. To the residue ethyl acetate (100 mL) and 0.1 M HCl (10 mL) were added, the phases were separated and organic phase was washed with brine (5 mL), dried over Na$_2$SO$_4$, filtered and the solvent evaporated under reduced pressure to obtain product **23a** (456 mg) as an off-white solid. Yield 90% (158 mg); mp 160–164 °C; ^{1}H NMR (400 MHz, DMSO-d_6) δ 3.30 (s, 3H, CH$_3$), 6.03 (s, 2H, NH$_2$), 6.55 (d, 2H, J = 8.7 Hz, Ar–H), 7.67 (d, 2H, J = 8.7 Hz, Ar–H), 11.50 (s, 1H, NH).

4.1.39. 4-Amino-N-(N,N-dimethylsulfamoyl)benzamide (23b)

To a solution of compound **22a** (0.692 mg, 2.531 mmol) in methanol (50 mL) under argon Pd–C (200 mg) was added and the reaction mixture was stirred under hydrogen atmosphere for 15 h. The catalyst was filtered off and the solvent was removed under reduced pressure. To the crude product ether (10 mL) was added, the suspension was sonicated and the solid was filtered off, washed with ether (5 mL) and dried to obtain product **23b** (585 mg) as a white solid. Yield 95% (585 mg); mp 130–134 °C; IR (ATR) ν = 3480, 3380, 3278, 2947, 1667, 1628, 1600, 1567, 1523, 1446, 1417, 1401, 1330, 1255, 1181, 1149, 1089, 978, 947, 892, 831, 809 cm^{-1}. ^{1}H NMR (400 MHz, DMSO-d_6) δ 2.78 (s, 6H, 2 × CH$_3$), 5.83 (s, 2H, NH$_2$), 6.52 (d, 2H, J = 8.7 Hz, Ar–H), 7.66 (d, 2H, J = 8.7 Hz, Ar–H), 11.11 (s, 1H, NH); ^{13}C NMR (100 MHz, DMSO-d_6) δ 38.16 (CH$_3$), 112.32, 119.97, 130.30, 152.62, 166.45 (C=O); MS (ESI) m/z (%) = 242.1 ([M − H]$^-$), HRMS for C$_9$H$_{12}$N$_3$O$_3$S: calculated 242.0599,

found 242.0597.

4.1.40. General procedure F. Synthesis of compounds 26a and 26b (with 26a as an example)

To a solution of 4-chlorophenol (**24**, 1.00 g, 7.78 mmol), methyl (*R*)-lactate (**25a**, 0.736 mL, 7.07 mmol) and triphenylphosphine (2.23 g, 8.48 mmol) in dry dichloromethane (25 mL) diisopropyl azodicarboxylate (1.72 mL, 8.48 mmol) was added dropwise and the mixture was stirred at rt for 3 h. The solvent was removed under reduced pressure and the residue was purified with flash column chromatography using ethyl acetate/petroleum ether (1:10 to 1:5) as solvent, to obtain **26a** (1.44 g) as a colourless oil.

4.1.41. Methyl (S)-2-(4-chlorophenoxy)propanoate (26a) [67]

Synthesized according to General procedure F. Colourless oil; yield 95% (1.44 g); [α]$_D^{25}$ − 49.2 (*c* 0.299, DMF); ^{1}H NMR (400 MHz, DMSO-d_6) δ 1.51 (d, 3H, J = 6.8 Hz, CH$_3$), 3.68 (s, 3H, OCH$_3$), 5.01 (q, 1H, J = 6.8 Hz, CH), 6.92 (d, 2H, J = 9.1 Hz, Ar–H), 7.33 (d, 2H, J = 9.1 Hz, Ar–H).

4.1.42. General procedure G. Synthesis of compounds 27a and 27b (with 27a as an example)

To a solution of compound **26a** (1.52 g, 7.08 mmol) in a mixture of methanol (10 mL) and water (2 mL) 2 M LiOH (5.31 mL, 10.6 mmol) was added dropwise and the mixture was stirred at rt for 15 h. The solvent was removed under reduced pressure, to the residue ethyl acetate (20 mL) and 0.5 M HCl (20 mL) were added, the phases were separated, organic phase was washed with 0.5 M HCl (20 mL) and brine (10 mL), dried over Na$_2$SO$_4$, filtered and the solvent evaporated under reduced pressure to obtain **27a** (1.20 g) as white crystals.

4.1.43. (S)-2-(4-Chlorophenoxy)propanoic acid (27a) [67,68]

Synthesized according to General procedure G. White crystals; yield 84% (1.20 g); mp 85–89 °C; [α]$_D^{25}$ − 64.4 (*c* 0.354, DMF); ^{1}H NMR (400 MHz, DMSO-d_6) δ 1.50 (d, 3H, J = 6.8 Hz, CH$_3$), 4.85 (q, 1H, J = 6.8 Hz, CH), 6.90 (d, 2H, J = 9.2 Hz, Ar–H), 7.33 (d, 2H, J = 9.2 Hz, Ar–H), 13.08 (s, 1H, COOH).

4.1.44. 4,5-Dibromo-N-(4-((methylsulfonyl)carbamoyl)phenyl)-1-phenyl-1H-pyrrole-2-carboxamide (29a)

Synthesized according to General procedure E from **3d** (88 mg, 0.256 mmol) and **23a** (50 mg, 0.233 mmol). Off-white solid; yield 22% (28 mg); mp 122–125 °C; IR (ATR) ν = 3251, 2933, 1662, 1593, 1525, 1497, 1420, 1321, 1245, 1155, 1073, 967, 894, 840, 763, 744 cm^{-1}. ^{1}H NMR (400 MHz, DMSO-d_6) δ 3.36 (s, 3H, CH$_3$), 7.26–7.37 (m, 2H, Ar–H), 7.45 (s, 1H, pyrr-H), 7.45–7.54 (m, 3H, Ar–H), 7.71 (d, 2H, J = 8.9 Hz, Ar–H), 7.89 (d, 2H, J = 8.9 Hz, Ar–H), 10.33 (s, 1H, NH), 12.00 (s, 1H, NH); ^{13}C NMR (100 MHz, acetone-d_6) δ 41.77 (CH$_3$), 100.03, 113.42, 116.85, 119.67, 119.75, 127.37, 129.07, 129.71, 129.81, 130.22, 139.96, 144.52, 158.06, 166.10; MS (ESI) m/z (%) = 537.9 ([M − H]$^-$), HRMS for C$_{19}$H$_{14}$N$_3$O$_4$SBr$_2$: calculated 537.9072, found 537.9082; HPLC: Phenomenex Luna 5 μm C18 column (4.6 mm × 150 mm); mobile phase: 30–90% acetonitrile in TFA (0.1%) in 16 min, 90% acetonitrile to 20 min; flow rate 1.0 mL/min; injection volume: 10 μL; retention time: 12.305 min (97.1% at 280 nm).

4.1.45. 1-Benzyl-4,5-dibromo-N-(4-((methylsulfonyl)carbamoyl)phenyl)-1H-pyrrole-2-carboxamide (29b)

Synthesized according to General procedure E from **3e** (30 mg, 0.084 mmol) and **23a** (18 mg, 0.084 mmol). White solid; yield 99% (46 mg); mp 229–231 °C; IR (ATR) ν = 3295, 3231, 3099, 3049, 2941, 1660, 1607, 1589, 1521, 1505, 1436, 1408, 1342, 1324, 1303, 1255, 1234, 1189, 1165, 1092, 974, 896, 842 cm^{-1}. ^{1}H NMR (400 MHz, DMSO-d_6) δ 3.37 (s, 3H, CH$_3$), 5.76 (s, 2H, CH$_2$), 7.00–7.06 (m, 2H, Ar–H), 7.24–7.27 (m, 1H, Ar–H), 7.31–7.35 (m, 2H, Ar–H), 7.45 (s, 1H, pyrr-H), 7.81 (d, 2H, J = 8.9 Hz, Ar–H), 7.93 (d, 2H, J = 8.9 Hz, Ar–H), 10.33 (s, 1H, NH),

12.02 (s, 1H, NH); ^{13}C NMR (100 MHz, DMSO-d_6) δ 41.35 (CH$_3$), 50.42 (CH$_2$), 98.29, 112.67, 116.69, 119.08, 126.07, 126.11, 127.17, 127.23, 128.58, 129.49, 137.29, 143.19, 158.22 (C=O), 165.67 (C=O); MS (ESI) m/z (%) = 551.9 ([M − H]$^-$), HRMS for C$_{20}$H$_{16}$N$_3$O$_4$SBr$_2$: calculated 551.9228, found 551.9219; HPLC: Phenomenex Luna 5 μm C18 column (4.6 mm × 150 mm); mobile phase: 30–90% acetonitrile in TFA (0.1%) in 16 min, 90% acetonitrile to 20 min; flow rate 1.0 mL/min; injection volume: 10 μL; retention time: 9.607 min (99.8% at 280 nm).

4.1.46. 1-(4-Chlorobenzyl)-N-(4-((methylsulfonyl)carbamoyl)phenyl)-1H-pyrrole-2-carboxamide (29c)

Synthesized according to General procedure E from **3c** (60 mg, 0.256 mmol) and **23a** (50 mg, 0.233 mmol). Off-white solid; yield 47% (47 mg); mp 212–216 °C; IR (ATR) ν = 3278, 3017, 2938, 1676, 1648, 1601, 1594, 1522, 1506, 1492, 1458, 1439, 1417, 1401, 1322, 1253, 1178, 1079, 1017, 981, 893, 845 cm^{-1}. ^{1}H NMR (400 MHz, DMSO-d_6) δ 3.36 (s, 3H, CH$_3$), 5.61 (s, 2H, CH$_2$), 6.23 (dd, 1H, J = 4.0, 2.6 Hz, pyrr-H), 7.13 (d, 2H, J = 8.5 Hz, Ar–H), 7.17 (dd, 1H, J = 4.0, 1.7 Hz, pyrr-H), 7.28 (dd, 1H, J = 2.6, 1.7 Hz, pyrr-H), 7.38 (d, 2H, J = 8.5 Hz, Ar–H), 7.81 (d, 2H, J = 8.9 Hz, Ar–H), 7.92 (d, 2H, J = 8.9 Hz, Ar–H), 10.10 (s, 1H, NH), 11.99 (s, 1H, NH); ^{13}C NMR (100 MHz, DMSO-d_6) δ 41.35 (CH$_3$), 50.33 (CH$_2$), 107.84, 115.40, 118.87, 124.29, 125.66, 128.36, 128.51, 129.35, 129.42, 131.66, 138.30, 143.72, 159.72, 165.77; MS (ESI) m/z (%) = 430.0 ([M − H]$^-$), HRMS for C$_{20}$H$_{17}$N$_3$O$_4$SCl: calculated 430.0628, found 430.0634; HPLC: Phenomenex Luna 5 μm C18 column (4.6 mm × 150 mm); mobile phase: 30–90% acetonitrile in TFA (0.1%) in 16 min, 90% acetonitrile to 20 min; flow rate 1.0 mL/min; injection volume: 10 μL; retention time: 11.455 min (98.0% at 280 nm).

4.1.47. 1-(4-Chlorobenzyl)-N-(4-((N,N-dimethylsulfamoyl)carbamoyl)phenyl)-1H-pyrrole-2-carboxamide (29d)

Synthesized according to General procedure E from **3c** (50 mg, 0.212 mmol) and **23b** (52 mg, 0.212 mmol). White solid; yield 67% (66 mg); mp 145–148 °C; IR (ATR) ν = 3327, 2938, 1687, 1657, 1608, 1592, 1519, 1439, 1457, 1441, 1413, 1342, 1327, 1315, 1281, 1255, 1240, 1169, 1084, 1017, 977, 892, 833 cm^{-1}. ^{1}H NMR (400 MHz, DMSO-d_6) δ 2.88 (s, 6H, 2 × CH$_3$), 5.60 (s, 2H, CH$_2$), 6.23 (dd, 1H, J = 4.0, 2.6 Hz, pyrr-H), 7.13 (d, 2H, J = 8.5 Hz, Ar–H), 7.17 (dd, 1H, J = 4.0, 1.7 Hz, pyrr-H), 7.28 (dd, 1H, J = 2.6, 1.7 Hz, pyrr-H), 7.37 (d, 2H, J = 8.5 Hz, Ar–H), 7.80 (d, 2H, J = 8.9 Hz, Ar–H), 7.90 (d, 2H, J = 8.9 Hz, Ar–H), 10.08 (s, 1H, NH), 11.67 (s, 1H, NH); ^{13}C NMR (100 MHz, DMSO-d_6) δ 37.92 (CH$_3$), 50.33 (CH$_2$), 107.83, 115.36, 118.88, 124.28, 125.57, 128.36, 128.52, 129.32, 131.66, 138.29, 143.52, 159.72, 165.08, signals for two carbons overlapping; MS (ESI) m/z (%) = 461.1 (MH$^+$), HRMS for C$_{21}$H$_{22}$N$_4$O$_4$SCl: calculated 461.1050, found 461.1051; HPLC: Phenomenex Luna 5 μm C18 column (4.6 mm × 150 mm); mobile phase: 30–90% acetonitrile in TFA (0.1%) in 16 min, 90% acetonitrile to 20 min; flow rate 1.0 mL/min; injection volume: 10 μL; retention time: 12.473 min (98.3% at 280 nm).

4.1.48. N-(4-((N,N-Dimethylsulfamoyl)carbamoyl)phenyl)benzofuran-2-carboxamide (30)

Synthesized according to General procedure E from benzofuran-2-carboxylic acid (**28**, 70 mg, 0.432 mmol) and **23b** (105 mg, 0.432 mmol). White solid; yield 24% (40 mg); mp 185–188 °C; IR (ATR) ν = 3333, 2940, 1685, 1661, 1595, 1578, 1537, 1522, 1502, 1474, 1432, 1403, 1342, 1306, 1277, 1247, 1188, 1206, 1167, 1108, 1086, 1075, 976, 953, 889, 841 cm^{-1}. ^{1}H NMR (400 MHz, DMSO-d_6) δ 2.90 (s, 6H, 2 × CH$_3$), 7.37–7.43 (m, 1H, Ar–H), 7.52–7.56 (m, 1H, Ar–H), 7.75 (dd, 1H, J = 8.4, 1.0 Hz, Ar–H), 7.85–7.87 (m, 2H, Ar–H), 7.97 (s, 4H, Ar–H), 10.84 (s, 1H, NH), 11.74 (s, 1H, NH); ^{13}C NMR (100 MHz, DMSO-d_6) δ 37.93 (CH$_3$), 111.37, 112.00, 119.54, 123.06, 123.95, 126.72, 127.02, 127.43, 129.41, 142.56, 148.28, 154.52, 156.93, 165.10; MS (ESI) m/z (%) = 388.1 (MH$^+$), HRMS for C$_{18}$H$_{18}$N$_3$O$_5$S: calculated 388.0967, found 388.0960; HPLC: Phenomenex Luna 5 μm C18 column (4.6 mm × 150 mm); mobile phase: 30–90% acetonitrile in TFA (0.1%) in 16 min, 90% acetonitrile to 20 min; flow rate 1.0 mL/min; injection volume: 10 μL; retention time: 9.616 min (95.3% at 280 nm).

4.1.49. N-(Methylsulfonyl)-4-((1R,2R)-2-phenylcyclopropane-1-carboxamido)benzamide (31a)

Synthesized according to General procedure E from **11a** (166 mg, 1.03 mmol) and **23a** (200 mg, 0.933 mmol). Off-white solid; yield 33% (110 mg); mp 222–226 °C; IR (ATR) ν = 3255, 3107, 2886, 1664, 1597, 1537, 1448, 1414, 1402, 1342, 1317, 1261, 1192, 1155, 1091, 1028, 960, 941, 893, 841 cm-1 [α]$_D^{25}$ +1.28 (c 0.313, DMF); ^{1}H NMR (400 MHz, DMSO-d_6) δ 1.40–1.47 (m, 1H, CH), 1.51–1.57 (m, 1H, CH), 2.08–2.14 (m, 1H, CH), 2.38–2.44 (m, 1H, CH), 3.37 (s, 3H, CH$_3$), 7.17–7.25 (m, 3H, Ar–H), 7.28–7.35 (m, 2H, Ar–H), 7.73 (d, 2H, J = 8.9 Hz, Ar–H), 7.92 (d, 2H, J = 8.9 Hz, Ar–H), 10.63 (s, 1H, NH), 11.99 (s, 1H, NH); ^{13}C NMR (100 MHz, DMSO-d_6) δ 15.86 (CH$_2$), 25.40 (CH), 26.89 (CH), 41.36 (CH$_3$), 118.01, 125.59, 125.90, 126.19, 128.36, 129.72, 140.52, 143.50, 165.64, 170.51; MS (ESI) m/z (%) = 359.1 (MH$^+$), HRMS for C$_{18}$H$_{19}$N$_2$O$_4$S: calculated 359.1066, found 359.1065; HPLC: Phenomenex Luna 5 μm C18 column (4.6 mm × 150 mm); mobile phase: 30–90% acetonitrile in TFA (0.1%) in 16 min, 90% acetonitrile to 20 min; flow rate 1.0 mL/min; injection volume: 10 μL; retention time: 8.888 min (99.1% at 280 nm).

4.1.50. N-(N,N-Dimethylsulfamoyl)-4-((1R,2R)-2-phenylcyclopropane-1-carboxamido)benzamide (31b)

Synthesized according to General procedure E from **11a** (50 mg, 0.308 mmol) and **23b** (75 mg, 0.308 mmol). White solid; yield 49% (58 mg); mp 208–212 °C; IR (ATR) ν = 3251, 3110, 3063, 2948, 2901, 1659, 1596, 1536, 1498, 1456, 1437, 1411, 1357, 1316, 1260, 1198, 1157, 1101, 1081, 1027, 973, 982, 949, 808 cm-1 [α]$_D^{25}$ − 1.46 (c 0.236, DMF); ^{1}H NMR (400 MHz, DMSO-d_6) δ 1.39–1.47 (m, 1H, CH), 1.51–1.55 (m, 1H, CH), 2.06–2.15 (m, 1H, CH), 2.38–2.44 (m, 1H, CH), 2.88 (s, 6H, 2 × CH$_3$), 7.15–7.25 (m, 3H, Ar–H), 7.28–7.33 (m, 2H, Ar–H), 7.71 (d, 2H, J = 8.8 Hz, Ar–H), 7.90 (d, 2H, J = 8.8 Hz, Ar–H), 10.60 (s, 1H, NH), 11.67 (s, 1H, NH); ^{13}C NMR (100 MHz, DMSO-d_6) δ 15.87 (CH$_2$), 25.36 (CH), 26.87 (CH), 37.91 (CH$_3$), 117.99, 125.74, 125.89, 126.19, 128.36, 129.60, 140.53, 143.24, 165.06, 170.46; MS (ESI) m/z (%) = 388.1 (MH$^+$), HRMS for C$_{19}$H$_{22}$N$_3$O$_4$S: calculated 388.1331, found 388.1337; HPLC: Phenomenex Luna 5 μm C18 column (4.6 mm × 150 mm); mobile phase: 30–90% acetonitrile in TFA (0.1%) in 16 min, 90% acetonitrile to 20 min; flow rate 1.0 mL/min; injection volume: 10 μL; retention time: 10.063 min (99.1% at 280 nm).

4.1.51. 4-(2-(3,4-Difluorophenyl)cyclopropane-1-carboxamido)-N-(methylsulfonyl)benzamide (31c)

Synthesized according to General procedure E from **11b** (50 mg, 0.252 mmol) and **23a** (54 mg, 0.252 mmol). White solid; yield 49% (49 mg); mp 228–232 °C; IR (ATR) ν = 3350, 3252, 3151, 3110, 2895, 1666, 1598, 1539, 1519, 1452, 1410, 1342, 1327, 1316, 1260, 1223, 1190, 1157, 1119, 1095, 1043, 973, 892 cm^{-1}. ^{1}H NMR (400 MHz, DMSO-d_6) δ 1.41–1.58 (m, 2H, 2 × CH), 2.07–2.12 (m, 1H, CH), 2.41–2.47 (m, 1H, CH), 3.37 (s, 3H, CH$_3$), 7.05–7.15 (m, 1H, Ar–H), 7.29–7.42 (m, 2H, Ar–H), 7.72 (d, 2H, J = 8.9 Hz, Ar–H), 7.92 (d, 2H, J = 8.9 Hz, Ar–H), 10.63 (s, 1H, NH), 11.99 (s, 1H, NH); ^{13}C NMR (100 MHz, DMSO-d_6) δ 15.89, 24.49, 27.06, 41.34 (s, CH$_3$), 114.93 (d, J_{C-F} = 17.4 Hz, Ar-C-2'), 117.26 (d, J_{C-F} = 16.8 Hz, Ar-C-5'), 118.04 (s, Ar-C-2,6), 122.84 (dd, J_{C-F} = 6.4, 3.3 Hz, Ar-C-6'), 125.70, 129.72 (s, Ar-C-3,5), 138.60 (dd, J_{C-F} = 6.4, 3.5 Hz, Ar-C-1'), 143.41, 147.96 (dd, J_{C-F} = 243, 12.6 Hz, Ar-C-4'), 149.38 (dd, J_{C-F} = 244, 12.5 Hz, Ar-C-3'), 165.66 (s, C=O), 170.16 (s, C=O); MS (ESI) m/z (%) = 393.1 ([M − H]$^-$), HRMS for C$_{18}$H$_{15}$N$_2$O$_4$SF$_2$: calculated 393.0721, found 393.0727; HPLC: Phenomenex Luna 5 μm C18 column (4.6 mm × 150 mm); mobile phase: 30–90% acetonitrile in TFA (0.1%) in 16 min, 90% acetonitrile to 20 min; flow rate 1.0 mL/min; injection volume: 10 μL; retention time: 9.726 min (99.6% at 280 nm).

4.1.52. (S)-4-(2-(4-Chlorophenoxy)propanamido)-N-(methylsulfonyl) benzamide (32a)

Synthesized according to General procedure E from **27a** (70 mg, 0.349 mmol) and **23a** (75 mg, 0.349 mmol). Off-white solid; yield 45% (62 mg); mp 180–183 °C; IR (ATR) ν = 3285, 3031, 2933, 1678, 1599, 1529, 1489, 1432, 1401, 1327, 1237, 1170, 1135, 1075, 1048, 972, 895, 822 cm-1 $[\alpha]_D^{25}$ − 43.9 (c 0.262, DMF); ^{1}H NMR (400 MHz, DMSO-d_6) δ 1.56 (d, 3H, J = 6.5 Hz, CHC$\underline{H}_3$), 3.37 (s, 3H, SO$_2$CH$_3$), 4.93 (q, 1H, J = 6.5 Hz, C$\underline{H}$CH$_3$), 6.99 (d, 2H, J = 8.9 Hz, Ar–H), 7.36 (d, 2H, J = 8.9 Hz, Ar–H), 7.76 (d, 2H, J = 8.8 Hz, Ar–H), 7.93 (d, 2H, J = 8.8 Hz, Ar–H), 10.49 (s, 1H, NH), 12.03 (s, 1H, NH); ^{13}C NMR (100 MHz, DMSO-d_6) δ 18.42 (CH$\underline{C}$H$_3$), 41.36 (SO$_2$CH$_3$), 73.93 ($\underline{C}$HCH$_3$), 116.84, 118.86, 124.96, 126.36, 129.36, 129.58, 142.72, 155.98, 165.62, 170.28; MS (ESI) m/z (%) = 395.1 ([M − H]$^-$), HRMS for C$_{17}$H$_{16}$N$_2$O$_5$SCl: calculated 395.0468, found 395.0462; HPLC: Phenomenex Luna 5 μm C18 column (4.6 mm × 150 mm); mobile phase: 30–90% acetonitrile in TFA (0.1%) in 16 min, 90% acetonitrile to 20 min; flow rate 1.0 mL/min; injection volume: 10 μL; retention time: 9.607 min (99.8% at 280 nm).

4.1.53. (R)-4-(2-(4-Chlorophenoxy)propanamido)-N-(methylsulfonyl) benzamide (32b)

Synthesized according to General procedure E from **27b** (50 mg, 0.249 mmol) and **23a** (53 mg, 0.249 mmol). White solid; yield 61% (60 mg); mp 180–183 °C; IR (ATR) ν = 3256, 3197, 2983, 2934, 1674, 1608, 1594, 1536, 1489, 1440, 1412, 1402, 1343, 1325, 1284, 1241, 1165, 1104, 1088, 1048, 1008, 976, 898, 854, 829, 820 cm-1 $[\alpha]_D^{25}$ +43.3 (c 0.261, DMF); ^{1}H NMR (400 MHz, DMSO-d_6) δ 1.56 (d, 3H, J = 6.6 Hz, CHC$\underline{H}_3$), 3.37 (s, 3H, SO$_2$CH$_3$), 4.93 (q, 1H, J = 6.6 Hz, C$\underline{H}$CH$_3$), 6.99 (d, 2H, J = 9.0 Hz, Ar–H), 7.36 (d, 2H, J = 9.0 Hz, Ar–H), 7.76 (d, 2H, J = 9.0 Hz, Ar–H), 7.93 (d, 2H, J = 9.0 Hz, Ar–H), 10.49 (s, 1H, NH), 12.03 (s, 1H, NH); ^{13}C NMR (100 MHz, DMSO-d_6) δ 18.42 (CH$\underline{C}$H$_3$), 41.36 (CH$_3$), 73.93 (CH), 116.84, 118.86, 124.97, 126.38, 129.36, 129.58, 142.71, 155.98, 165.63 (C=O), 170.28 (C=O); MS (ESI) m/z (%) = 395.0 ([M − H]$^-$), HRMS for C$_{17}$H$_{16}$N$_2$O$_5$SCl: calculated 395.0468, found 395.0461; HPLC: Phenomenex Luna 5 μm C18 column (4.6 mm × 150 mm); mobile phase: 30–90% acetonitrile in TFA (0.1%) in 16 min, 90% acetonitrile to 20 min; flow rate 1.0 mL/min; injection volume: 10 μL; retention time: 9.616 min (99.1% at 280 nm).

4.1.54. (R)-4-(2-(4-Chlorophenoxy)propanamido)-N-(N,N-dimethylsulfamoyl)benzamide (32c)

Synthesized according to General procedure E from **27b** (44 mg, 0.219 mmol) and **23b** (53 mg, 0.219 mmol). White solid; yield 32% (30 mg); mp 162–164 °C; IR (ATR) ν = 3482, 3313, 2987, 2938, 1687, 1597, 1526, 1489, 1442, 1408, 1346, 1333, 1280, 1236, 1167, 1086, 975, 895, 846, 817 cm-1 $[\alpha]_D^{25}$ +39.0 (c 0.181, DMF); ^{1}H NMR (400 MHz, DMSO-d_6) δ 1.56 (d, 3H, J = 6.5 Hz, CHC$\underline{H}_3$), 2.87 (s, 6H, 2 × CH$_3$), 4.92 (q, 1H, J = 6.5 Hz, C$\underline{H}$CH$_3$), 6.99 (d, 2H, J = 9.0 Hz, Ar–H), 7.36 (d, 2H, J = 9.0 Hz, Ar–H), 7.74 (d, 2H, J = 8.8 Hz, Ar–H), 7.91 (d, 2H, J = 8.8 Hz, Ar–H), 10.46 (s, 1H, NH), 11.71 (s, 1H, NH); ^{13}C NMR (100 MHz, DMSO-d_6) δ 18.41 (CH$\underline{C}$H$_3$), 37.93 (NCH$_3$), 73.95 ($\underline{C}$HCH$_3$), 116.86, 118.83, 124.95, 126.70, 129.36, 129.45, 142.39, 155.98, 165.11, 170.22; MS (ESI) m/z (%) = 424.1 ([M − H]$^-$), HRMS for C$_{18}$H$_{19}$N$_3$O$_5$SCl: calculated 424.0734, found 424.0730; HPLC: Phenomenex Luna 5 μm C18 column (4.6 mm × 150 mm); mobile phase: 30–90% acetonitrile in TFA (0.1%) in 16 min, 90% acetonitrile to 20 min; flow rate 1.0 mL/min; injection volume: 10 μL; retention time: 10.772 min (99.6% at 280 nm).

4.1.55. ((1R,2R)-2-Phenylcyclopropyl)methanol (33) [69]

To a solution of lithium aluminium hydride (152 mg, 4.01 mmol) in dry THF (10 mL) cooled on an ice bath a solution of (1R,2R)-2-phenyl-cyclopropane-1-carboxylic acid (**11a**, 0.500 g, 3.08 mmol) in dry THF (5 mL) was added dropwise and the mixture was allowed to warm to rt. After 5 h the mixture was treated with water and 2 M NaOH, the layers were separated and the water phase was extracted with ethyl acetate (3

× 20 mL). The combined organic phase was dried with Na$_2$SO$_4$, filtered and the solvent removed under reduced pressure to afford **33** (411 mg) as a colourless oil. Yield 90% (411 mg). $[\alpha]_D^{25}$ − 16.2 (c 0.457, DMF); ^{1}H NMR (400 MHz, DMSO-d_6) δ 0.81–0.89 (m, 2H, CH$_2$), 1.23–1.31 (m, 1H, CH), 1.76–1.80 (m, 1H, CH), 3.33–3.40 (m, 1H, CH), 3.43–3.49 (m, 1H, CH), 4.62 (t, 1H, J = 5.6 Hz, OH), 7.05–7.14 (m, 3H, Ar–H), 7.21–7.27 (m, 2H, Ar–H).

4.1.56. General procedure H. Synthesis of compounds 34a and 34b (with 34a as an example)

To a solution of methyl 3-hydroxybenzoate (312 mg, 2.05 mmol) and triphenylphosphine (0.808 g, 3.08 mmol) in dry THF (20 mL) compound **33** (0.500 g, 3.08) and DEAD (1.69 mL, 3.70 mmol) were added consecutively. The mixture was stirred at rt for 3 h and then heated at 50 °C for 15 h. The solvent was removed under reduced pressure and the residue was purified with flesh column chromatography using ethyl acetate/petroleum ether (1:10) as solvent, to obtain **34a** (290 mg) as a pink oil.

4.1.57. Methyl 3-(((1R,2R)-2-phenylcyclopropyl)methoxy)benzoate (34a)

Synthesized according to general procedure H. Pink oil, yield 50% (290 mg); IR (ATR) ν = 3026, 2951, 1719, 1601, 1585, 1489, 1445, 1416, 1329, 1275, 1218, 1189, 1099, 1076, 1023, 993, 904, 875 cm-1 $[\alpha]_D^{25}$ − 1.64 (c 0.293, DMF); ^{1}H NMR (400 MHz, DMSO-d_6) δ 0.99–1.10 (m, 2H, CH$_2$), 1.51–1.63 (m, 1H, CH), 1.97–2.02 (m, 1H, CH), 3.85 (s, 3H, CH$_3$), 3.98–4.11 (m, 2H, CH$_2$O), 7.07–7.17 (m, 3H, Ar–H), 7.21–7.28 (m, 3H, Ar–H), 7.40–7.46 (m, 2H, Ar–H), 7.51–7.57 (m, 1H, Ar–H); ^{13}C NMR (100 MHz, DMSO-d_6) δ 13.92 (CH$_2$), 21.20 (CH), 21.93 (CH), 52.18 (CH$_3$), 71.15 (CH$_2$O), 114.25, 120.00, 121.35, 125.47, 125.61, 128.23, 129.93, 130.90, 142.27, 158.56, 166.03 (C=O); MS (ESI) m/z (%) = 305.1 (MNa$^+$), HRMS for C$_{18}$H$_{18}$O$_3$Na: calculated 305.1154, found 305.1157.

4.1.58. General procedure I. Synthesis of compounds 36a and 36b (with 36a as an example)

To a solution of compound **35a** (100 mg, 0.372 mmol) in dry dichloromethane (5 mL) oxalyl chloride (2 M solution in dichloromethane, 0.410 mL, 0.818 mmol) was added and the mixture was stirred at rt for 15 h. The solvent was removed under reduced pressure and to the residue dry tetrahydrofuran (5 mL) was added to obtain solution A. In a separate flask, compound **21a** (71 mg, 0.745 mmol) was dissolved in dry tetrahydrofuran (15 mL) and to the obtained solution sodium hydride (403 mg, 10.5 mmol, 60% dispersion in mineral oil) was added portionwise at 0 °C. After 30 min solution A was added dropwise and the mixture was stirred for 1 h at rt and for 15 h at 50 °C. The solvent was removed under reduced pressure and to the residue ethyl acetate (30 mL) and 0.5 M HCl (10 mL) were added. The layers were separated, the organic phase was washed with 0.5 M HCl (2 × 10 mL) and brine (10 mL), dried over Na$_2$SO$_4$, filtered and evaporated under reduced pressure. To the solid residue ether (10 mL) was added, the suspension was sonicated, the solid was filtered off, washed with ether and dried to obtain **35a** (35 mg) as a white solid.

4.1.59. N-(Methylsulfonyl)-3-(((1R,2R)-2-phenylcyclopropyl)methoxy) benzamide (36a)

Synthesizes according to general procedure I. White solid; yield 27% (35 mg); mp 128–132 °C; IR (ATR) ν = 3292, 3033, 2935, 1687, 1603, 1586, 1500, 1421, 1404, 1376, 1324, 1269, 1222, 1169, 1160, 1094, 1059, 1031, 1013, 999, 947, 880, 860, 814, 756 cm-1 $[\alpha]_D^{25}$ +1.23 (c 0.309, DMF); ^{1}H NMR (400 MHz, DMSO-d_6) δ 0.99–1.14 (m, 2H, CH$_2$), 1.51–1.66 (m, 1H, CH), 1.95–2.07 (m, 1H, CH), 3.38 (s, 3H, CH$_3$), 4.00–4.14 (m, 2H, OCH$_2$), 7.07–7.19 (m, 3H, Ar–H), 7.19–7.33 (m, 3H, Ar–H), 7.43 (t, 1H, J = 8.1 Hz, Ar–H), 7.49–7.56 (m, 2H, Ar–H), 12.12 (s, 1H, NH); ^{13}C NMR (100 MHz, DMSO-d_6) δ 13.90 (CH$_2$), 21.24 (CH), 21.93 (CH), 41.26 (OCH$_2$), 71.26 (CH$_3$), 113.42, 120.14, 120.72,

125.49, 125.63, 128.24, 129.76, 132.85, 142.24, 158.45, 166.05; MS (ESI) *m/z* (%) = 344.1 ([M − H]⁻), HRMS for $C_{18}H_{18}NO_4S$: calculated 344.0957, found 344.0947; HPLC: Phenomenex Luna 5 μm C18 column (4.6 mm × 150 mm); mobile phase: 30–90% acetonitrile in TFA (0.1%) in 16 min, 90% acetonitrile to 20 min; flow rate 1.0 mL/min; injection volume: 10 μL; retention time: 11.811 min (95.8% at 280 nm).

4.1.60. N-(Methylsulfonyl)-4-(((1R,2R)-2-phenylcyclopropyl)methoxy) benzamide (36b)

Synthesizes according to general procedure I from **35b** (150 mg, 0.559 mmol). White solid; yield 30% (58 mg); mp 98–99 °C; IR (ATR) ν = 3254, 3030, 2931, 2866, 1692, 1668, 1603, 1577, 1510, 1498, 1434, 1417, 1396, 1372, 1335, 1318, 1247, 1177, 1153, 1123, 1076, 1032, 997, 969, 890, 852, 839 cm-1 $[\alpha]_D^{25}$ +25.4 (*c* 0.221, DMF); ¹H NMR (400 MHz, DMSO-d_6) δ 0.99–1.13 (m, 2H, CH_2), 1.54–1.67 (m, 1H, CH), 1.96–2.07 (m, 1H, CH), 3.37 (s, 3H, CH_3), 4.04–4.16 (m, 2H, OCH_2), 7.06 (d, 2H, *J* = 8.9 Hz, Ar–H), 7.10–7.20 (m, 3H, Ar–H), 7.23–7.30 (m, 2H, Ar–H), 7.93 (d, 2H, *J* = 8.9 Hz, Ar–H), 11.94 (s, 1H, NH); ¹³C NMR (100 MHz, DMSO-d_6) δ 13.99 (CH_2), 21.21 (CH), 21.78 (CH), 41.39 (OCH_2), 71.34 (CH_3), 114.32, 123.51, 125.51, 125.63, 128.25, 130.64, 142.19, 162.46, 165.61; MS (ESI) *m/z* (%) = 424.1 ([M − H]⁻), HRMS for $C_{18}H_{18}NO_4S$: calculated 344.0957, found 344.0958; HPLC: Phenomenex Luna 5 μm C18 column (4.6 mm × 150 mm); mobile phase: 30–90% acetonitrile in TFA (0.1%) in 16 min, 90% acetonitrile to 20 min; flow rate 1.0 mL/min; injection volume: 10 μL; retention time: 11.598 min (98.9% at 280 nm).

Declaration of competing interest

The authors declare that they have no known competing financial interests or personal relationships that could have appeared to influence the work reported in this paper.

Data availability

Data will be made available on request.

Appendix A. Supplementary data

Supplementary data to this article can be found online at https://doi.org/10.1016/j.ejmech.2023.115530.

Abbreviations

ATCC   American type culture collection
Boc   *tert*-butyloxycarbonyl
BOB   (benzotriazol-1-yloxy)tris(dimethylamino)phosphonium hexafluorophosphate
DIAD   diisopropyl azodicarboxylate
DMF   *N,N*-dimethylformamide
ESI   electrospray ionization
HepG2   human hepatocellular carcinoma cell line

K_v channel   voltage-gated potassium channel
NMM   *N*-methylmorpholine
TBTU   *N,N,N′,N′*-tetramethyl-O-(benzotriazol-1-yl)uronium tetrafluoroborate
TFA   trifluoroacetic acid
THF   tetrahydrofuran

References

[1] W.A. Catterall, G. Wisedchaisri, N. Zheng, The conformational cycle of a prototypical voltage-gated sodium channel, Nat. Chem. Biol. 16 (2020) 1314–1320.
[2] L. Xu, X. Ding, T. Wang, S. Mou, H. Sun, T. Hou, Voltage-gated sodium channels: structures, functions, and molecular modeling, Drug Discov. Today 24 (2019) 1389–1397.
[3] S.K. Bagal, B.E. Marron, R.M. Owen, R.I. Storer, N.A. Swain, Voltage gated sodium channels as drug discovery targets, Channels 9 (2015) 360–366.
[4] M.D. Ruiz, R.L. Kraus, Voltage-gated sodium channels: structure, function, pharmacology, and clinical indications, J. Med. Chem. 58 (2015) 7093–7118.
[5] H.Z. Shen, D.L. Liu, K. Wu, J.L. Lei, N. Yan, Structures of human Nav1.7 channel in complex with auxiliary subunits and animal toxins, Science 363 (2019) 1303–1308.
[6] G. Goodwin, S.B. McMahon, The physiological function of different voltage-gated sodium channels in pain, Nat. Rev. Neurosci. 22 (2021) 263–274.
[7] M.H. Meisler, S.F. Hill, W.X. Yu, Sodium channelopathies in neurodevelopmental disorders, Nat. Rev. Neurosci. 22 (2021) 152–166.
[8] H.B. Yu, M. Li, W.P. Wang, X.L. Wang, High throughput screening technologies for ion channels, Acta Pharmacol. Sin. 37 (2016) 34–43.
[9] A. Mathie, E.L. Veale, R.G. Holden, Heterologous expression of ion channels in mammalian cell lines, Methods Mol. Biol. 2188 (2021) 51–65.
[10] J. Payandeh, T. Scheuer, N. Zheng, W.A. Catterall, The crystal structure of a voltage-gated sodium channel, Nature 475 (2011) 353–358.
[11] J. Payandeh, T.M.G. El-Din, T. Scheuer, N. Zheng, W.A. Catterall, Crystal structure of a voltage-gated sodium channel in two potentially inactivated states, Nature 486 (2012) 135–139.
[12] X. Zhang, W.L. Ren, P. DeCaen, C.Y. Yan, X. Tao, L. Tang, J.J. Wang, K. Hasegawa, T. Kumasaka, J.H. He, J.W. Wang, D.E. Clapham, N. Yan, Crystal structure of an orthologue of the NaChBac voltage-gated sodium channel, Nature 486 (2012) 130–134.
[13] E.C. McCusker, C. Bagneris, C.E. Naylor, A.R. Cole, N. D'Avanzo, C.G. Nichols, B. A. Wallace, Structure of a bacterial voltage-gated sodium channel pore reveals mechanisms of opening and closing, Nat. Commun. 3 (2012) 1102.
[14] C. Bagneris, P.G. DeCaen, C.E. Naylor, D.C. Pryde, I. Nobeli, D.E. Clapham, B. A. Wallace, Prokaryotic NavMs channel as a structural and functional model for eukaryotic sodium channel antagonism, Proc. Natl. Acad. Sci. U. S. A. 111 (2014) 8428–8433.
[15] H.Z. Shen, Q. Zhou, X.J. Pan, Z.Q. Li, J.P. Wu, N. Yan, Structure of a eukaryotic voltage-gated sodium channel at near-atomic resolution, Science 355 (2017), eaal4326.
[16] X.J. Li, F. Xu, H. Xu, S.L. Zhang, Y.W. Gao, H.W. Zhang, Y.L. Dong, Y.C. Zheng, B. Yang, J.Y. Sun, X.C. Zhang, Y. Zhao, D.H. Jiang, Structural basis for modulation of human Na(V)1.3 by clinical drug and selective antagonist, Nat. Commun. 13 (2022) 1286.
[17] S. Ahuja, S. Mukund, L. Deng, K. Khakh, E. Chang, H. Ho, S. Shriver, C. Young, S. Lin, J.P. Johnson Jr., P. Wu, J. Li, M. Coons, C. Tam, B. Brillantes, H. Sampang, K. Mortara, K.K. Bowman, K.R. Clark, A. Estevez, Z. Xie, H. Verschoof, M. Grimwood, C. Dehnhardt, J.C. Andrez, T. Focken, D.P. Sutherlin, B.S. Safina, M. A. Starovasnik, D.F. Ortwine, Y. Franke, C.J. Cohen, D.H. Hackos, C.M. Koth, J. Payandeh, Structural basis of Nav1.7 inhibition by an isoform-selective small-molecule antagonist, Science 350 (2015) aac5464.
[18] A.M. Tan, O.A. Samad, S.D. Dib-Hajj, S.G. Waxman, Virus-mediated knockdown of Nav1.3 in dorsal root ganglia of STZ-induced diabetic rats alleviates tactile allodynia, Mol. Med. 21 (2015) 544–552.
[19] O.A. Samad, A.M. Tan, X.Y. Cheng, E. Foster, S.D. Dib-Hajj, S.G. Waxman, Virus-mediated shRNA knockdown of Nav1.3 in rat dorsal root ganglion attenuates nerve injury-induced neuropathic pain, Mol. Ther. 21 (2013) 49–56.
[20] B.C. Hains, J.P. Klein, C.Y. Saab, M.J. Craner, J.A. Black, S.G. Waxman, Upregulation of sodium channel Nav1.3 and functional involvement in neuronal hyperexcitability associated with central neuropathic pain after spinal cord injury, J. Neurosci. 23 (2003) 8881–8892.
[21] R.Y. Yin, D. Liu, M. Chhoa, C.M. Li, Y. Luo, M.S. Zhang, S.G. Lehto, D.C. Immke, B. D. Moyer, Voltage-gated sodium channel function and expression in injured and uninjured rat dorsal root ganglia neurons, Int. J. Neurosci. 126 (2016) 182–192.
[22] C.S. Cheah, R.E. Westenbroek, W.H. Roden, F. Kalume, J.C. Oakley, L.A. Jansen, W. A. Catterall, Correlations in timing of sodium channel expression, epilepsy, and sudden death in Dravet syndrome, Channels 7 (2013) 468–472.
[23] X.H. He, Y. Zang, X. Chen, R.P. Pang, J.T. Xu, X.A. Zhou, X.H. Wei, Y.Y. Li, W. J. Xin, Z.H. Qin, X.G. Liu, TNF-alpha contributes to up-regulation of Nav1.3 and Nav1.8 in DRG neurons following motor fiber injury, Pain 151 (2010) 266–279.
[24] M. Poffers, N. Buhne, C. Herzog, A. Thorenz, R. Chen, F. Guler, A. Hage, A. Leffler, F. Echtermeyer, Sodium channel Nav1.3 is expressed by polymorphonuclear neutrophils during mouse heart and kidney ischemia in vivo and regulates

adhesion, transmigration, and chemotaxis of human and mouse neutrophils in vitro, Anesthesiology 128 (2018) 1151–1166.

[25] T. Zaman, K.L. Helbig, J. Clatot, C.H. Thompson, S.K. Kang, K. Stouffs, A.E. Jansen, L. Verstraete, A. Jacquinet, E. Parrini, R. Guerrini, Y. Fujiwara, S. Miyatake, B. Ben-Zeev, H. Bassan, O. Reish, D. Marom, N. Hauser, T.A. Vu, S. Ackermann, C. E. Spencer, N. Lippa, S. Srinivasan, A. Charzewska, D. Hoffman-Zacharska, D. Fitzpatrick, V. Harrison, P. Vasudevan, S. Joss, D.T. Pilz, K.A. Fawcett, I. Helbig, N. Matsumoto, J.A. Kearney, A.E. Fry, E.M. Goldberg, SCN3A-related neurodevelopmental disorder: a spectrum of epilepsy and brain malformation, Ann. Neurol. 88 (2020) 348–362.

[26] T. Zaman, I. Helbig, I.B. Bozovic, S.D. DeBrosse, A.C. Bergqvist, K. Wallis, L. Medne, A. Maver, B. Peterlin, K.L. Helbig, X. Zhang, E.M. Goldberg, Mutations in SCN3A cause early infantile epileptic encephalopathy, Ann. Neurol. 83 (2018) 703–717.

[27] T. Zaman, I. Helbig, I.B. Božović, S.D. Debrosse, A.C. Bergqvist, K. Wallis, L. Medne, A. Maver, B. Peterlin, K.L. Helbig, X. Zhang, E.M. Goldberg, Mutations in SCN3A cause early infantile epileptic encephalopathy, Ann. Neurol. 83 (2018) 703–717.

[28] C.G. Vanoye, C.A. Gurnett, K.D. Holland, A.L. George, J.A. Kearney, Novel SCN3A variants associated with focal epilepsy in children, Neurobiol. Dis. 62 (2014) 313–322.

[29] J.V. Mulcahy, H. Pajouhesh, J.T. Beckley, A. Delwig, J. Du Bois, J.C. Hunter, Challenges and opportunities targeting the voltage-gated sodium channel isoform Nav1.7, J. Med. Chem. 62 (2019) 8695–8710.

[30] K. McCormack, S. Santos, M.L. Chapman, D.S. Krafte, B.E. Marron, C.W. West, M. J. Krambis, B.M. Antonio, S.G. Zellmer, D. Printzenhoff, K.M. Padilla, Z. Lin, P. K. Wagoner, N.A. Swain, P.A. Stupple, M. de Groot, R.P. Butt, N.A. Castle, Voltage sensor interaction site for selective small molecule inhibitors of voltage-gated sodium channels, Proc. Natl. Acad. Sci. U. S. A. 110 (2013) E2724–E2732.

[31] S. Sun, Q. Jia, A.Y. Zenova, M.S. Wilson, S. Chowdhury, T. Focken, J. Li, S. Decker, M.E. Grimwood, J.C. Andrez, I. Hemeon, T. Sheng, C.A. Chen, A. White, D. H. Hackos, L. Deng, G. Bankar, K. Khakh, E. Chang, R. Kwan, S. Lin, K. Nelkenbrecher, B.D. Sellers, A.G. DiPasquale, J. Chang, J. Pang, L. Sojo, A. Lindgren, M. Waldbrook, Z. Xie, C. Young, J.P. Johnson, C.L. Robinette, C. J. Cohen, B.S. Safina, D.P. Sutherlin, D.F. Ortwine, C.M. Dehnhardt, Identification of selective acyl sulfonamide-cycloalkylether inhibitors of the voltage-gated sodium channel Nav1.7 with potent analgesic activity, J. Med. Chem. 62 (2019) 908–927.

[32] B.S. Safina, S.J. McKerrall, S. Sun, C.A. Chen, S. Chowdhury, Q. Jia, J. Li, A. Y. Zenova, J.C. Andrez, G. Bankar, P. Bergeron, J.H. Chang, E. Chang, J. Chen, R. Dean, S.M. Decker, A. DiPasquale, T. Focken, I. Hemeon, K. Khakh, A. Kim, R. Kwan, A. Lindgren, S. Lin, J. Maher, J. Mezeyova, D. Misner, K. Nelkenbrecher, J. Pang, R. Reese, S.D. Shields, L. Sojo, T. Sheng, H. Verschoof, M. Waldbrook, M. S. Wilson, Z. Xie, C. Young, T.S. Zabka, D.H. Hackos, D.F. Ortwine, A.D. White, J. P. Johnson Jr., C.L. Robinette, C.M. Dehnhardt, C.J. Cohen, D.P. Sutherlin, Discovery of acyl-sulfonamide Nav1.7 inhibitors GDC-0276 and GDC-0310, J. Med. Chem. 64 (2021) 2953–2966.

[33] A.J. Roecker, M.E. Layton, J.E. Pero, M.J. Kelly 3rd, T.J. Greshock, R.L. Kraus, Y. Li, R. Klein, M. Clements, C. Daley, A. Jovanovska, J.E. Ballard, D. Wang, F. Zhao, A.P.J. Brunskill, X. Peng, X. Wang, H. Sun, A.K. Houghton, C.S. Burgey, Discovery of arylsulfonamide Nav1.7 inhibitors: IVIVC, MPO methods, and optimization of selectivity profile, ACS Med. Chem. Lett. 12 (2021) 1038–1049.

[34] W. Wu, Z. Li, G. Yang, M. Teng, J. Qin, Z. Hu, L. Hou, L. Shen, H. Dong, Y. Zhang, J. Li, S. Chen, J. Tian, J. Zhang, L. Ye, The discovery of tetrahydropyridine analogs as hNav1.7 selective inhibitors for analgesia, Bioorg. Med. Chem. Lett 27 (2017) 2210–2215.

[35] N.A. Swain, D. Batchelor, S. Beaudoin, B.M. Bechle, P.A. Bradley, A.D. Brown, B. Brown, K.J. Butcher, R.P. Butt, M.L. Chapman, S. Denton, D. Ellis, S.R.G. Galan, S.M. Gaulier, B.S. Greener, M.J. de Groot, M.S. Glossop, I.K. Gurrell, J. Hannam, M. S. Johnson, Z. Lin, C.J. Markworth, B.E. Marron, D.S. Millan, S. Nakagawa, A. Pike, D. Printzenhoff, D.J. Rawson, S.J. Ransley, S.M. Reister, K. Sasaki, R.I. Storer, P. A. Stupple, C.W. West, Discovery of clinical candidate 4-[2-(5-Amino-1*H*-pyrazol-4-yl)-4-chlorophenoxy]-5-chloro-2-fluoro-*N*-1,3-thiazol-4 -ylbenzenesulfonamide (PF-05089771): design and optimization of diaryl ether aryl sulfonamides as selective inhibitors of Nav1.7, J. Med. Chem. 60 (2017) 7029–7042.

[36] T.J. Kornecook, R. Yin, S. Altmann, X. Be, V. Berry, C.P. Ilch, M. Jarosh, D. Johnson, J.H. Lee, S.G. Lehto, J. Ligutti, D. Liu, J. Luther, D. Matson, D. Ortuno, J. Roberts, K. Taborn, J. Wang, M.M. Weiss, V. Yu, D.X.D. Zhu, R.T. Fremeau Jr., B. D. Moyer, Pharmacologic characterization of AMG8379, a potent and selective small molecule sulfonamide antagonist of the voltage-gated sodium channel Nav1.7, J. Pharmacol. Exp. Therapeut. 362 (2017) 146–160.

[37] J. Payandeh, D.H. Hackos, Selective ligands and drug discovery targeting the voltage-gated sodium channel Nav1.7, Handb. Exp. Pharmacol. 246 (2018) 271–306.

[38] E.C. Emery, A.P. Luiz, J.N. Wood, Nav1.7 and other voltage-gated sodium channels as drug targets for pain relief, Expert Opin. Ther. Targets 20 (2016) 975–983.

[39] K. Kingwell, Nav1.7 Withholds its Pain Potential, Nat Rev Drug Discov, 2019.

[40] D.C. Pryde, N.A. Swain, P.A. Stupple, C.W. West, B. Marron, C.J. Markworth, D. Printzenhoff, Z. Lin, P.J. Cox, R. Suzuki, S. McMurray, G.J. Waldron, C.E. Payne, J.S. Warmus, M.L. Chapman, The discovery of a potent Nav1.3 inhibitor with good oral pharmacokinetics, MedChemComm 8 (2017) 1255–1267.

[41] A.B.J. Fulp, Matthew Scott, Christopher John Markworth, Brian Edward Marron, Darrick Conway Duncan, Christopher West, Xiaodong Wang, Shulan Zhou, From PCT Int. Appl, 2009. WO 2009012242 A2 20090122.

[42] M. McGann, FRED pose prediction and virtual screening accuracy, J. Chem. Inf. Model. 51 (2011) 578–596.

[43] M. McGann, FRED and HYBRID docking performance on standardized datasets, J. Comput. Aided Mol. Des. 26 (2012) 897–906.

[44] Jesus E. Gonzales III, Andreas P. Termin, Esther Martinborough, Nicole Zimmerman, From PCT Int. Appl\, 2005. WO 2005013914 A2 20050217.

[45] M. Rogers, N. Zidar, D. Kikelj, R.W. Kirby, Characterization of endogenous sodium channels in the ND7-23 neuroblastoma cell line: implications for use as a heterologous ion channel expression system suitable for automated patch clamp screening, Assay Drug Dev. Technol. 14 (2016) 109–130.

[46] V.N. Uebele, S.K. England, A. Chaudhary, M.M. Tamkun, D.J. Snyders, Functional differences in Kv1.5 currents expressed in mammalian cell lines are due to the presence of endogenous Kv beta 2.1 subunits, J. Biol. Chem. 271 (1996) 2406–2412.

[47] S. Peigneur, C.D. Oliveira, F.C.D. Fonseca, K.L. McMahon, A. Mueller, O. Cheneval, A.C.N. Freitas, H. Starobova, I.D.G. Duarte, D.J. Craik, I. Vetter, M.E. de Lima, C. I. Schroeder, J. Tytgat, Small cyclic sodium channel inhibitors, Biochem. Pharmacol. 183 (2021).

[48] T. Sterling, J.J. Irwin, ZINC 15-ligand discovery for everyone, J. Chem. Inf. Model. 55 (2015) 2324–2337.

[49] P.C.D. Hawkins, A.G. Skillman, G.L. Warren, B.A. Ellingson, M.T. Stahl, Conformer generation with OMEGA: algorithm and validation using high quality structures from the protein databank and cambridge structural database, J. Chem. Inf. Model. 50 (2010) 572–584.

[50] P.C.D. Hawkins, A.G. Skillman, A. Nicholls, Comparison of shape-matching and docking as virtual screening tools, J. Med. Chem. 50 (2007) 74–82.

[51] J.A. Grant, M.A. Gallardo, B.T. Pickup, A fast method of molecular shape comparison: a simple application of a Gaussian description of molecular shape, J. Comput. Chem. 17 (1996) 1653–1666.

[52] J.A. Grant, B.T. Pickup, A Gaussian description of molecular shape, J Phys Chem-Us 99 (1995) 3503–3510.

[53] S. Kearnes, V. Pande, ROCS-derived features for virtual screening, J. Comput. Aided Mol. Des. 30 (2016) 609–617.

[54] R. Pingaew, P. Mandi, C. Nantasenamat, S. Prachayasittikul, S. Ruchirawat, V. Prachayasittikul, Design, synthesis and molecular docking studies of novel *N*-benzenesulfonyl-1,2,3,4-tetrahydroisoquinoline-based triazoles with potential anticancer activity, Eur. J. Med. Chem. 81 (2014) 192–203.

[55] F. Bilodeau, M.C. Brochu, N. Guimond, K.H. Thesen, P. Forgione, Palladium-catalyzed decarboxylative cross-coupling reaction between heteroaromatic carboxylic acids and aryl halides, J. Org. Chem. 75 (2010) 1550–1560.

[56] D.A. Shirley, B.H. Gross, P.A. Roussel, Metalation of pyrrole, 1-methylpyrrole, and 1-phenylpyrrole with normal-butyllithium, J. Org. Chem. 20 (1955) 225–231.

[57] C. Ouairy, P. Michel, B. Delpech, D. Crich, C. Marazano, Synthesis of *N*-acyl-5-aminopenta-2,4-dienals via base-induced ring-opening of *N*-acylated furfurylamines: scope and limitations, J. Org. Chem. 75 (2010) 4311–4314.

[58] B. Mochona, L. Le, M. Gangapuram, N. Mateeva, T. Ardley, K.K. Redda, Synthesis of 2-(*N*-benzylpyrrolyl)-benzimidazoles using polyphosphoric acid prompted cyclocondensation, J. Heterocycl. Chem. 47 (2010) 1367–1371.

[59] Mark S. Chambers, Victor G. Matassa, Stephen R. Fletcher, From U.S, Benzodiazepine Derivatives as Antagonists of Cholecystokinin and Gastrin, Compositions Containing Them and Their Use in Therapy, US, 1994, 5360802 A 19941101.

[60] C.R. Reddy, B. Mahipal, S.R. Yaragorla, A new and efficient method for the facile synthesis of *N*-acyl sulfonamides under Lewis acid catalysis, Tetrahedron Lett. 48 (2007) 7528–7532.

[61] M.A. Altmeyer, A. Marschner, R. Schiffmann, C.D. Klein, Subtype-selectivity of metal-dependent methionine aminopeptidase inhibitors, Bioorg. Med. Chem. Lett 20 (2010) 4038–4044.

[62] A.G. Sams, G.K. Mikkelsen, M. Larsen, M. Langgard, M.E. Howells, T.J. Schroder, L. T. Brennum, L. Torup, E.B. Jorgensen, C. Bundgaard, M. Bang-Andersen, Discovery of phosphoric acid mono-{2-[(E/Z)-4-(3,3-dimethyl-butyrylamino)-3,5-difluorobenzoylimino]-thiazol-3-ylmethyl} ester (Lu AA47070): a phosphonooxymethylene prodrug of a potent and selective hA(2A) receptor antagonist, J. Med. Chem. 54 (2011) 751–764.

[63] J. Picha, V. Vanek, M. Budesinsky, J. Mladkova, T.A. Garrow, J. Jiracek, The development of a new class of inhibitors for betaine-homocysteine *S*-methyltransferase, Eur. J. Med. Chem. 65 (2013) 256–275.

[64] Nuria Aguilar, et al., Preparation of substituted tricyclic compounds with activity towards EP1 receptors, PCT Int. Appl. (2013), 2013149997.

[65] M.N.S. Rad, A. Khalafi-Nezhad, Z. Asrari, S. Behrouz, Highly efficient one-pot synthesis of N-acylsulfonamides using cyanuric chloride at room temperature, Synthesis-Stuttgart (2010) 2599–2603.

[66] T. Nittoli, K. Curran, S. Insaf, M. Di-Grandi, M. Orlowski, R. Chopra, A. Agarwal, A. Y.M. Howe, A. Prashad, M.B. Floyd, B. Johnson, A. Sutherland, K. Wheless, B. Feld, J. O'Connell, T.S. Mansour, J. Bloom, Identification of anthranilic acid derivatives as a novel class of allosteric inhibitors of hepatitis C NS5B polymerase, J. Med. Chem. 50 (2007) 6290-6290.

[67] G. Kirchner, M.P. Scollar, A.M. Klibanov, Resolution of racemic mixtures via lipase catalysis in organic-solvents, J. Am. Chem. Soc. 107 (1985) 7072–7076.

[68] M. Schmittel, A.A. Mahajan, G. Bucher, J.W. Bats, Thermal C-2-C-6 cyclization of enyne-allenes. Experimental evidence for a stepwise mechanism and for an unusual thermal silyl shift, J. Org. Chem. 72 (2007) 2166–2173.